

Republic of Iraq
Ministry of Higher Education
University of Kerbala - College of Engineering
Department of Mechanical Engineering



Experimental and Theoretical Investigation on The Vibration of Epoxy - Carbon Tubes Conveying Fluid

A Thesis

Submitted to The Mechanical Engineering Department,
University of Kerbala in Partial Fulfillment for the Requirements of the
Degree of Master of Science in Mechanical Engineering
(Applied Mechanics)

By

Sarah Salim Hasan

B.Sc. In Mech. Eng. 2017

Supervised by

**Prof. Dr. Ahmed A. Al-Rajihy
Asst. Prof. Dr. Basim Raheem Sadeq**

2022 A.D.

١٤٤٣ هـ

بِسْمِ اللَّهِ الرَّحْمَنِ الرَّحِيمِ

الْحَمْدُ لِلَّهِ الَّذِي أَنزَلَ عَلَيْنَا الْكِتَابَ وَلَمْ يَجْعَلْ لَنَا غَوْلًا

قَبْلَ الْبَيْتِ بِأَنَّ شَاكِرًا مِنْ لَدُنْهِ وَيُبَشِّرَ الْمُؤْمِنِينَ الَّذِينَ

يَعْمَلُونَ الصَّالِحَاتِ أَنَّ لَهُمْ أَجْرًا حَسَنًا

صدق الله العلي العظيم

سورة الكهف (2,1)

Dedication

To my dear parents

To my family

To all my distinguished teachers

Sarah S. Al- Esawy

Acknowledgment

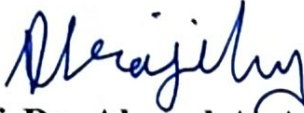
In the beginning, I would like to thank God for all this great blessing. The success of the result of this research takes much guidance and help from many people, and I am very fortunate to have had it all along with mastery of the research. All I did was just because of this guidance, and I will not forget to thank them.

I want to thank my supervisors **Prof. Dr. Ahmed A. Al-Rajihy** and **Asst. Prof. Dr. Basim Raheem Sadeq** for supervising this mission and their generosity, patience, and the constant guidance in all stages of the work. It was my great fortune to get their advice and guidance. Many thanks to the head of the Mechanical Engineering department **Asst. Prof. Dr. Haider J. kurji** and **Asst. Prof. Dr. Muhammad Wahab**, for providing the departments' facilities and continuous encouragement. It is my pleasure to receive continuous encouragement, support, and guidance from all members of the **Mechanical Engineering Department at Kerbala University**, which helped me complete my work successfully; many thanks for them.

Sarah S. Al- Esawy

Supervisor Certification

We certify that the thesis entitled " **Experimental and Theoretical Investigation on The Vibration of Epoxy – Carbon Tubes Conveying Fluid**" has been prepared by " **Sarah Salim Hasan** " under our supervision at the Department of Mechanical Engineering, College of Engineering, **University of Kerbala** as a partial fulfillment of the requirements for the Degree of Master of Science in Mechanical Engineering (**Applied mechanics**)

Signature: 
Name: Prof. Dr. Ahmed A. Al-Rajihy
Date: 10/ 2/ 2022

Signature: 
Name: Asst. Prof. Dr. Basim Raheem Sadeq
Date: 10/ 2 / 2022

Linguistic Certificate

I certify that the thesis entitled " **Experimental and Theoretical Investigation on The Vibration of Epoxy – Carbon Tubes Conveying Fluid**" submitted by " **Sarah Salim Hasan**" has been prepared under my linguistic supervision. Its language has been amended to meet the English style.

Signature: *Hazim U. Jamali*

Linguistic advisor: *Hazim Umran Jamali*

Date: *8/2/2022*

Examining Committee Certification

We certify that we have read this thesis entitled " Experimental and Theoretical Investigation on The Vibration of Epoxy – Carbon Tubes Conveying Fluid" and as an examining committee, examined the student " Sarah Salim Hasan" in its content and that in our opinion, it meets the standard of a thesis and is adequate for the award of the Degree of Master of Science in Mechanical Engineering / Applied Mechanics.

Signature: 
Name: Prof. Dr. Ahmed A. Al-Rajihy

Date: 10/ 2/ 2022
(Supervisor)

Signature: 
Name: Asst. Prof. Dr. Basim Raheem Sadeq

Date: 10/ 2/ 2022
(Supervisor)

Signature: 
Name: Asst. Prof. Dr. Amjad Al-Hamood

Date: 8/ 2/ 2022
(Member)

Signature: 
Name: Lecturer. Dr. Ahmed Abboodi Taher

Date: 13/ 2/ 2022
(Member)

Signature: 
Name: Prof. Dr. Basim Ajeel Abass

Date: 13/ 4/ 2022
(Chairman)

Approval of Mechanical Engineering Department

Signature: 
Name: Asst. Prof. Dr. Haider J. Kurji

(Head of the Mechanical Engineering Department)

Date: 14/ 2/ 2022

Approval of Deanery of the College of Engineering / University of Kerbala

Signature: 
Name: Prof. Dr. Laith Shakir Rasheed

(Dean of the College of Engineering)

Date: 14/ 2/ 2022

Abstract

Composite tubes are usually made of two or more laminated composite materials. These tubes can be used for fuel lines, hydraulic tubes, house and industrial uses.

In the current study, the most common types of composite materials will be used to manufacture the tube which is carbon fiber – epoxy. It is widely used due to its significant properties, including high strength to weight, good toughness and suitable prices.

Because of the tendency to use successful tubes with less vibration and low corrosion rate, this study is directed to the dynamical behavior of tube made of the composite material conveying fluid.

The effect of flow velocity and internal damping on free vibration of tube made of the composite material , which represents the main parameter in this work, is investigated using different types of boundary conditions.

A systematic evaluation of the fundamental aspects of the dynamic behavior of tube made of the composite material with the effect of flow velocity and internal damping on free vibration of tube made of the composite material , which represents the main parameter in this work, is investigated using different types of boundary conditions.

The mathematical model of tube made of the composite material is solved analytically to calculate the effect of the related parameters and variables. The theoretical results are presented in a dimensionless form for with the mechanical properties.

The natural frequency was determined in the theoretical part by deriving the governing equation using the Euler-Bernoulli theorem and substituting the boundary conditions into the equation to extract the roots of the polynomial equation and writing it in the form of a matrix consisting of four terms to be substituted in the (Q-basic) program to determine the value of the natural frequency.

It was found that increasing flow velocity causes the natural frequency to decrease gradually. The rate of decrease increased until the natural frequency value was nearly zero at point called "critical flow velocity" which is the flow velocity at which the natural frequency decreases. The simply supported composite tube has a dimensionless critical flow velocity of 3.12. In contrast, the clamped support tube has a dimensionless critical flow velocity of 6.23, and the dimensionless critical flow velocity for clamped-pinned is 4.42. These results were without the effect of internal damping.

According to the theoretical results , the critical flow velocity increased when the mode of vibration was increased. Furthermore, the critical flow velocity of a clamped composite tube is 50% higher than that critical flow velocity of simply supported composite tubes. The internal damping affects the natural frequency by up to 4.79 % when the internal damping increases by 0.01%.

In the experimental part, a device was manufactured to confirm the theoretical results of calculating the natural frequency by using the tachometer to determine the rotational speed of the crankshaft, where the number of revolutions displayed on the digital screen of the device represents the value of the experimental natural frequency of the tube made of composite materials and compare the experimental results with the theoretical results.

List of contents

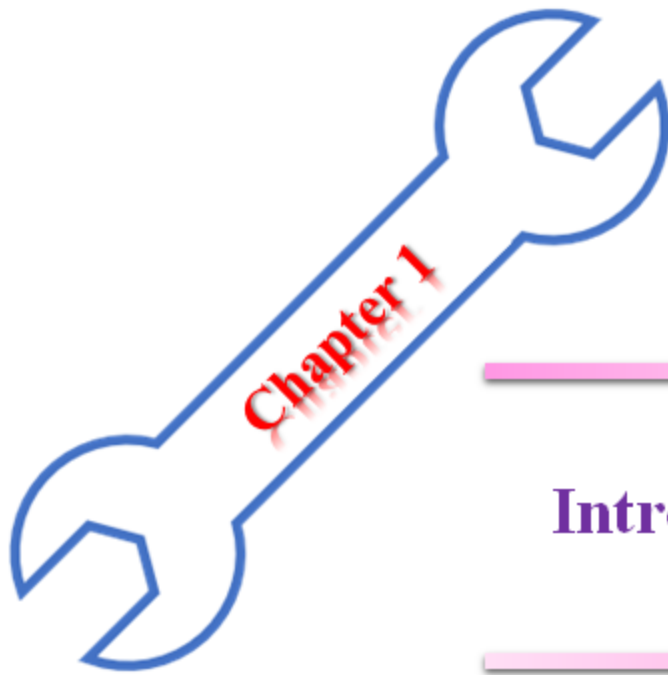
Subject	Page
Abstract	I
List of Contents	III
Nomenclature	V
Chapter One: Introduction	
1.1 General	1
1.2 Objectives	4
1.3 Thesis outline	4
Chapter Two : Literature review	
2.1 Introduction	5
2.2 Literature survey	5
2.2.1 Tube conveying fluid	5
2.2.2 Composite tube conveying fluid	10
2.2.3 Tube conveying fluid with the effect of Internal damping	15
2.3 Summary	17
Chapter Three :Mathematical Modelling	
3.1 Introduction	18
3.2 Materials and Methods	18
3.3 Vibration Analysis	24
3.3.1 Boundary conditions	25
3.3.2 Tube Natural Frequencies	28
Chapter Four :Experimental Work	
4.1 Introduction	31
4.2 Testing models	31

4.3 Test Rig	32
4.4 Vibration test	34
4.5 Modulus of Elasticity and Density of the tube	36
4.6 Calibration of Flowmeter	37
4.7 Experimental Natural Frequency Test	38
Chapter Five : Results and Discussion	
5.1 Introduction	39
5.2 Theoretical Results	39
5.2.1 Effect of flow velocity on the natural frequency	39
5.2.2 Effect of internal damping on the natural frequency	45
5.2.3 Effect of supporting types on the natural frequency	53
5.3 Experimental Results	55
Chapter Six : Conclusions and Work Suggestions	
6.1 Introduction	63
6.2 Conclusions	63
6.3 Future Work Suggestions	64
References	
References	65

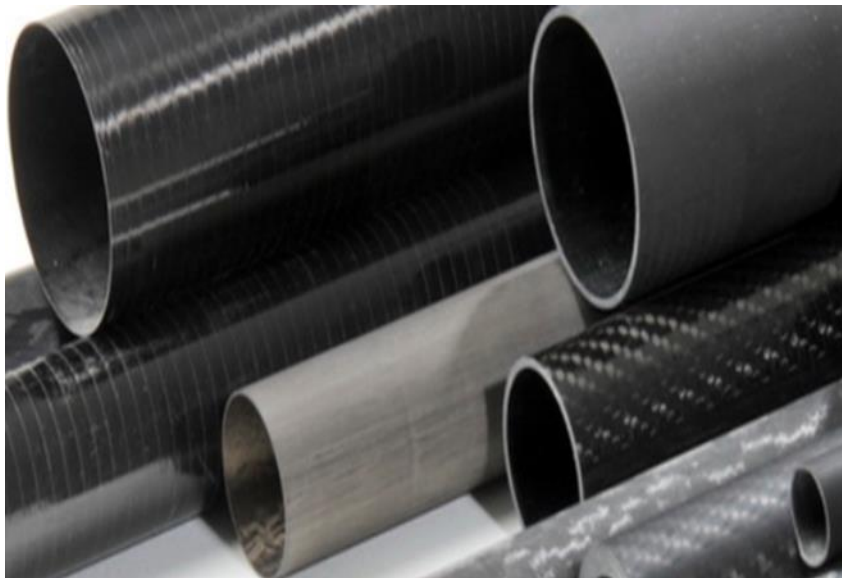
Nomenclatures

Symbol	Meaning	Units
A	Cross section area	m^2
a_f	Acceleration of the fluid	m^2/s
D_i	Tube internal diameter	m
D_o	Tube outer diameter	m
E	Modulus of elasticity	N/m^2
E^*	Internal damping coefficient	
E_c	Modulus of elasticity of composite materials of tube	N/m^2
E_F	Modulus of elasticity of fiber	N/m^2
E_M	Modulus of elasticity of the matrix	N/m^2
F	Normal force between fluid and tube per unit length	N/m
I	Second moment of area	m^4
L	Tube length	m
M	Bending moment	Nm
m_f	Fluid mass per unit length	kg/m
m_t	Tube mass per unit length	kg/m
ρ_t	Tube density per unit length	kg/m^3
P	Pressure	N/m^2
P_i	Internal pressure	N/m^2
Q	Fluid flow rate	l/min
q	Shear force per unit length	N/m
S	Tube's internal perimeter	m
T	Tension force in tube per unit length	N/m
t	Time	sec

U	Dimensionless fluid velocity	
V	Axial flow velocity	m/s
V_f	Lateral velocity of the fluid	m/s
V_F	Volume fraction of the fiber	
V_M	Volume fraction of the matrix	
x	Axial coordinate	
y	Lateral coordinate	
Greek symbols		
β	Fluid - tube mass ratio	
γ	Dimensionless pressure	
η	Dimensionless coordinate	
λ	Roots of the polynomial equation	
μ	Dimensionless internal damping coefficient	
ξ	Dimensionless coordinate	
τ	Dimensionless time	
Ω	Dimensionless circular frequency of oscillation	
ω	Natural frequency	Rad/sec



Introduction



Chapter One

Introduction

1.1 General

A composite material consists of the combination of two or more substances. This merging process leads to obtaining a new material with engineering and physical properties that differ from the properties of the materials in their composition. The general use of composite material depends largely on these materials' mechanical and physical properties, so studying these properties under the influence of forces and loads in different conditions acquires great importance to know the appropriateness of these properties for the place of work of these materials.

In industry, the reinforcement of resins with synthetic fibers is the most common. For the manufacture of composite material, two materials must be provided:

- (Matrix Material): The base material is polymeric materials, and it is the most widely used and widespread because of its good mechanical and thermal properties. Examples of polymeric materials are epoxy resin.
- (Reinforcing Material): Two main advantages must be available in such materials, which are high resistance and low ductility in order to be able to strengthen the base materials.

There are several methods of strengthening, and the most common is the strengthening of fibers due to their great strength compared to resin materials. The fibers are of different types and shapes, which are continuous or non-continuous.

In the current study, the most common types of composite materials will be used to manufacture the tube carbon fiber – epoxy, as shown in figure (1.1). It is widely used due to its significant properties, including high strength to weight and good toughness, as well as reasonable prices, as they are available in a variety of applications.

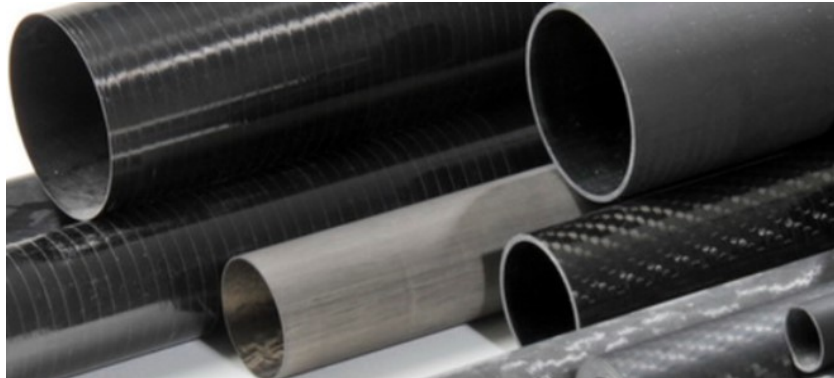


Figure (1.1). Carbon fiber tubes [2].

By identifying the advantages of tubes made of composite materials, the differences between metal tubes and tubes made of composite materials can be determined. With the increase of demand of tubes constructed from composite materials, there has been an upsurge in research related to the mechanics of composite tubes and predicting failure under different loading conditions. The composite tube offers several advantages over metallic systems, especially where control and mitigation regimes are not correctly followed. Metallic structures require more inspection, repair, and maintenance during their service life, meaning a need to schedule shutdowns while increasing expenditure. These shutdowns are mitigated against the composite tube to remove any corrosion-related problems.

Composite tubes also have a superior internal fluid flow performance compared to metallic tubes with a lack of scaling and other bore restriction issues. Composite tubes also demonstrate superb strength and stiffness with much less weight, making them easier to handle without lifting equipment, reducing lifecycle, transportation, and installation costs. However, composite materials can be more expensive than their metal counterparts, although the reduced assembly costs for composites can offset this cost.

Based on the preceding, it becomes clear the importance of tubes made of composite materials, as Composite tubes are already showing a track record of use for a range of applications across different industries. Already widely used for transporting different types of water, these tubes are increasingly used in the oil and gas industry, where their strength, lightweight, and lack of problems with corrosion are proving beneficial. Easy to transport and install, and with very little requirement for maintenance and inspection, the benefits of composite tubes balance out the increased cost of materials. Available in various material types and as spool-able, flexible options, composite tubes look set to continue rising.

Because of the tendency to use successful tubes with less vibration and low corrosion rate, this study and the previous studies are directed to the dynamical behavior of composite tubes conveying fluid. The effect of flow material damping and type of support on the free vibration of composite tubes represent the focus of the current study.

1.2 Objectives

The following points can summarize the main objectives of the present work;

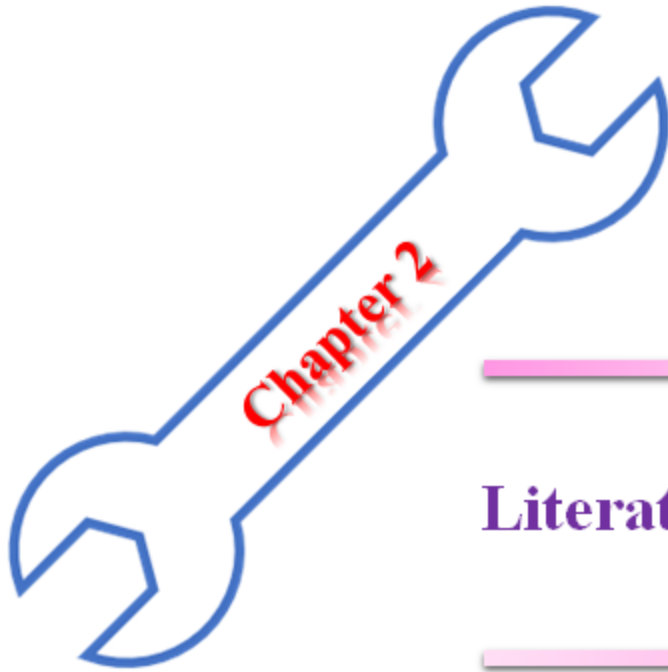
1. Investigation of the effect of flow velocity on free vibration of the tube made of composite material
2. Investigation of the effect of internal damping of tube material on the dynamical behavior of the tube.
3. Defining the values of resonance of the tube under investigation to prevent resonance problems such as mechanical failure.
4. Investigation the dynamics of behavior of tube with the effect of supporting type and the effect of adding intermediate support on free vibration of the tube made of composite material

1.3 Thesis outline

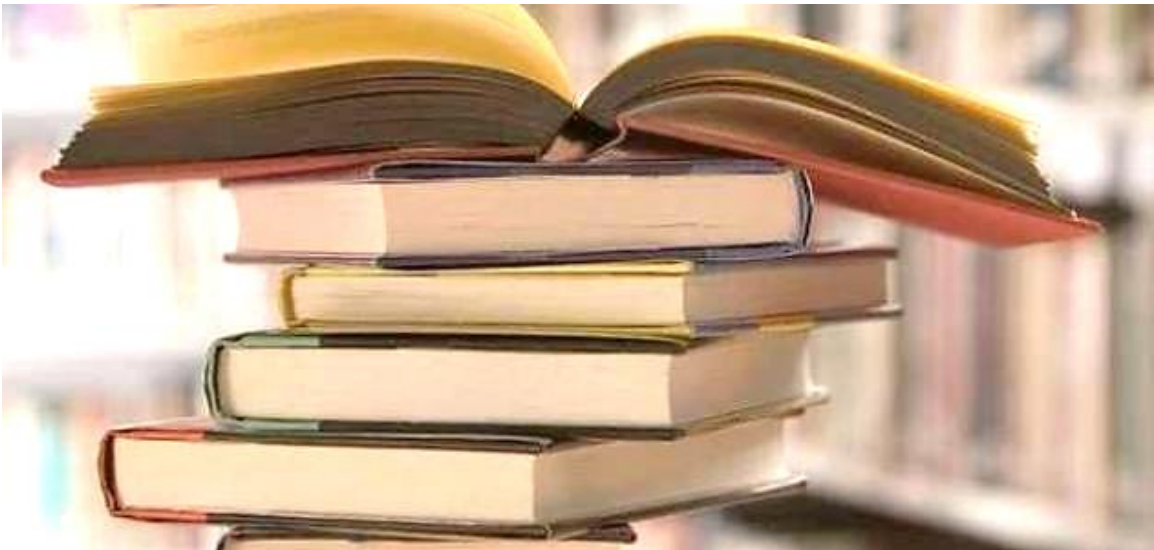
The chapters of this thesis are arranged in the following order:

The background for this work is presented in the first chapter to emphasize its relevance in the theoretical application and practical reality .The second chapter shows some prior studies that can apply some of the features and design of the topic .

The equation of motion for composite tubes that convey fluids, including the internal damping to determine the natural frequency necessary for composite tube vibration, is presented in the third chapter. The fourth chapter explains and clarifies the practical application and the equipment utilized. The fifth chapter provides the theoretical and experimental findings of the tests under different boundary conditions. Finally, the sixth chapter draws the topic conclusions.



Literature review



Chapter two

Literature review

2.1 Introduction

Pipelines for fluid conveying are important in various design applications because they have provided an important service on a large scale in a wide variety of industrial sectors to convey fluid. These tubes are utilized in various applications, water supply lines, and fuel conveying line drainage. Numerous researches have been undertaken to investigate the dynamic behavior of tubes made of various materials due to the large variety of systems that utilize tubes.

2.2 Literature survey

2.2.1 Tube conveying fluid

Paidoussis and Issid [2] investigated the dynamics and methods of stabilization of flexible tubes that convey fluids, assuming that the velocity is steady. Stability maps are presented for parametric instabilities, computed by Bolotin's method, for tubes with pinned or clamped ends, as well as for cantilevered tubes. It is found that the extent of the instability regions increases with flow velocity for clamped – clamped and pinned–pinned tubes. At the same time, a more complex behavior obtains in the case of cantilevered tubes. It is shown that conservative systems are subject to buckling (divergence) at sufficiently high flow velocities and oscillatory

instabilities (flutter) at higher flow velocities. In all cases, dissipation reduces the extent of or eliminates parametric instability zones.

Liu and Xuan [3] investigated the dynamic analysis of supported tubes conveying pulsating fluid in the Hamiltonian system using (Precise Integration Method) PIM, which is considered a practical way to investigate the dynamic analysis of tubes conveying fluid. To confirm this methodology, many pinned-pinned tubes were solved numerically using different velocities and frequencies.

Yi-min et al. [4] investigated the natural frequency of fluid-structure interaction in pipeline conveying fluid by the eliminated element-Galerkin method. The natural frequency equations with different boundary conditions are obtained. The characteristics of pipeline conveyed fluid, such as flow velocity, stiffness, mass, and length linked to the natural frequency, were investigated. The results indicate that the effect of Coriolis force on natural frequency is inappreciable. Then the relationship between the natural frequency of the pipeline conveying fluid and that of the Euler beam is analyzed.

Al-Rajihy and Alwan [5] investigated the vibrational characteristics of a Y-shaped tube conveying flowing fluid. The tube comprises 3- straight tube segments meet at the intermediate junction. The governing equation of straight tube conveying fluid is used with each of the three segments. The clamped free and clamped-pinned boundary conditions were discussed. The coupled effects of the type of boundary conditions, the angle between the two Y-segments, fluid velocity, and length ratio of segments on the dynamics of the tube are studied. The Y-tube loses its stability at flow velocity higher than the straight tube of the same characteristics.

Al-sahib et al. [6] focused their study on the vibration and stability of straight tubes made of ASTM-214-71 mild steel, conveying turbulent steady water with different velocities and boundary conditions. Single-pass fusion arc welding with appropriate parameters welded the tube on its mid-span. A new analytical model was derived from investigating the effects of residual stresses at girth welds of a tube on the vibration characteristics and stability. The reaction components of the residual stresses at a single pass girth weld in a tube were combined with a tensioned Euler-Bernoulli beam and plug flow model to investigate the effect of welding on the vibration characteristics of a tube. A finite element (FE) simulation was presented to evaluate the velocity and pressure distributions in a single-phase fluid flow. A prestressed modal analysis was employed to determine the vibration characteristics of a welded tube conveying fluid. Experimental work was carried out by building a rig mainly composed of different boundary conditions welded tubes conveying fluid and provided with the necessary measurement equipment is to fulfill the required investigations. It has been proven theoretically and experimentally that the residual stresses due to welding reduce natural frequencies for both clamped-clamped and clamped-pinned tube conveying fluid. Also, it proved that for small fluid velocity (sub-critical), the clamped-clamped and clamped-pinned welded tubes conveying fluid are stable for relatively high fluid velocities (super-critical).

Ismail [7] provided the analytical solutions to determine essential properties of conservative and non-conservative energy tubes conveying fluid, such as pressure, velocity, and mass ratio. With low rather than high flow rate pumps, a method for calculating the critical velocity has been provided. The findings revealed that the approach worked with conservative tubes, with a

5% error rate between theoretical and actual outcomes, and that non-conservative tubes required more sophisticated solutions.

Ritto et al. [8] discussed the problem of a tube conveying fluid of interest in several engineering applications, such as micro-systems or drill-string dynamics. The deterministic stability analysis developed by Paidoussis and Issid (1974) is extended to the case for which modeling errors in the computational model induce model uncertainties. The Euler-Bernoulli beam model is used to model the tube, and the plug flow model is used to take into account the internal flow in the tube. The resulting differential equation is discretized using the finite element method, and a reduced-order model is constructed from some eigenmodes of the beam. The numerical results show the random response of the system for different levels of uncertainty and the system's reliability for different dimensionless speeds and levels of uncertainty.

Kesimli et al. [9] discussed linear vibration of the fluid-carrying tube with intermediate support. Supports located at the ends of the tube were clamped supports. Support was located in the middle section show the features of simple support. It was accepted that the fluid velocity varied harmonically by an average speed. The equation of motion and limit conditions of the system were obtained using the Hamilton principle. The solutions were obtained using the Multiple Scale Method, one Perturbation Methods. The first term in the perturbation series causes the linear problem. Exact natural frequencies were calculated by the solution of the linear problem for the different positions of the support at the center, different longitudinal stiffness, different tube coefficient, different rate of fullness, and natural frequencies depending on the fluid's velocity exactly.

Al-Rajihy and Kadhom [10] focused on fluid velocity on the bending behavior of a cantilever tube under a lateral impact force. According to the results, increasing flow velocity lowers the amplitude of the bending moment's first reaction to the impact lateral force by approximately 9%. The findings take around 48% of the time to lower the amplitude of the bending moment response by 90%. The findings of this study indicate that fluid flow velocity has a substantial influence on the dynamic response of tubes conveying fluid.

A dynamic stability test of the tube conveying fluid with a linear spring was carried out by Alnomani [11]. The spring work produced good results for the system frequency utilizing the finite element analysis approach. The stiffness ratio of the tube is raised to improve the system's stability. The spring's position is determined by the tube's flow velocity and the spring's stability.

Sutar et al. [12] calculated the natural frequencies of fluid conveying tubes using (guided - simple, guided - clamped, guided - guided, and guided - free) boundary conditions. It is described how fluid flow velocity affects natural frequencies. The point of flutter is found by determining critical velocities. To simulate the tube, a Euler–Bernoulli beam is used. Hamilton's approach creates the differential equation of motion for free vibration. Muller's approximate technique is used to generate the natural frequency equation. There is a decrease in natural frequency as velocity increases for any boundary conditions.

2.2.2 Composite tube conveying fluid

The vibrational behavior of the tube made of composite material conveying fluid has been studied by many research.

Oke and Khulief [13] looked at how interior surface degradation influences the vibrational behavior of the tube made of composite material conveying fluid. The wave-based finite element approach is utilized to model and determine the faulty fluid tube system using the extended Hamilton principle. The modal characteristics of tube vibrations were calculated using the generalized eigenvalue problem. The suggested model was evaluated, and many standard solutions were used to verify the influence of inner wall thinning on the vibrational behavior of composite tubes conveying fluid. The obtained results make it possible to use the vibration signature as a basis for detecting internal corrosion defects in pipelines.

Szabó et al. [14] used a finite element model and practical testing to demonstrate the actual performance of a filament-wound composite tube bent three times. The composite reinforcement plies were characterized using the linear viscoelastic material model, included in the finite element model. The rubber liners were classified as a two-parameter model under the Mooney - Rivlin model. There is a high agreement between the modeling results and the experimental findings for three-point bending force-displacement curves.

Oke and Khulief [15] analyzed the dynamic response when fluid flows through a tube with an internal surface imperfection. The extended Hamilton's principle was used to derive equations of motion, while the wavelet-based finite element method (WBFEM) was used to discretize the equations. Internal surface flaws prolong the tube's length and have a cross-

section that changes radial and angular directions. Integrating the equations of motion using the MATLAB solver ODE45 yields the faulty tube's dynamic response. ANSYS was used to assess the dynamic model. Some benchmark findings show the impact of internal surface imperfections on the dynamic response of composite tubes conveying fluid.

Dai et al. [16] studied The dynamics of fluid-conveying cantilevered tubes consisting of two segments made of different materials, focusing on the effects of different length ratios between the two segments. Two kinds of hybrid tubes are considered: one is made of steel and aluminum, and the other is aluminum and epoxy. The complex frequency of the four lowest modes of the hybrid system is calculated in two representative cases for successively increasing flow velocity values to demonstrate how the transition from stability to instability occurs. Compared with a uniform tube conveying fluid, it is found that the hybrid tube is capable of displaying more complex and sometimes unexpected dynamical behaviors. The numerical results show that an instability–restabilization–instability sequence would occur in such a hybrid tube system as the flow velocity is successively increasing. When the length ratio between the two segments is successively increased, the lowest order of unstable modes may frequently shift from one to another. It is also demonstrated that the flutter instability first occurring in the fourth mode is possible with increasing flow velocity, and a certain unstable mode may suddenly regain stability.

Al - Raheimy [17] investigated the influence of several forms of support on the cross-sectional frequency of composite tubes with parameters of 1 m length, 1 mm thickness, and 1 cm inner radius, including clamped – free, clamped – clamped and clamped – pinned. The tube is made of fiberglass

and a polyester resin that has been solidified into a matrix. The fibers are of various lengths; the first is short but not connected, while the second is lengthy and continuous for a specific fiber section. The natural frequency decreases as the flow increases from zero to critical velocity. The length of the disconnected fiber determines the frequency rise. It has been concluded that the fiberglass tubes would have a low critical velocity and a low natural frequency than Kevlar fiber tubes.

Khudayarov et al. [18] investigated the Vibration problems of pipelines made of composite materials conveying pulsating flow of gas and fluid. A dynamic model of motion of pipelines conveying pulsating fluid flow supported by a Hetenyi's base is developed taking into account the viscosity properties of the structure material, axial forces, internal pressure and Winkler's viscoelastic base. To describe the processes of viscoelastic material strain, the Boltzmann–Volterra integral model with weakly singular hereditary kernels is used. Using the Bubnov–Galerkin method, the problem is reduced to the study of a system of ordinary integro-differential equations (IDE). A computational algorithm is developed based on the elimination of the features of IDE with weakly singular kernels, followed by the use of quadrature formulas. The effect of rheological parameters of the pipeline material, flow rate and base parameters on the vibration of a viscoelastic pipeline conveying pulsating fluid is analyzed. The convergence analysis of the approximate solution of the Bubnov–Galerkin method is carried out. It was revealed that the viscosity parameters of the material and the pipeline base lead to a significant change in the critical flow rate. It was stated that an increase in excitation coefficient of pulsating flow and the parameter of internal pressure leads to a decrease in the critical flow rate. It is shown that

an increase in the singularity parameter, the Winkler base parameter, the rigidity parameter of the continuous base layer and the Reynolds number increases the critical flow rate.

Geuchy and Hoa [19] studied the flexural stiffness of thick composite tubes. For thick composite tubes, a fiber placement machine was used automatically. The tubes were put through their paces using a different testing method. Stresses and flexural stiffness were measured using Both strain gages and Digital Image Correlation. The tubes' flexural stiffnesses during the bending experiment were measured. A comparison is made between the experimental results and those obtained using different equations.

Malawi et al. [20] developed a model that replicates the behavior of unidirectional fiber composite tubes made of the same material type. The modules are firmly connected to produce a separate axial grading tube for this purpose. Once the transfer matrix analysis was complete, the Levenberg - Marquardt method solved the resulting nonlinear equations with their complex roots. It was decided to make some handy diagrams. Because of this, the current design may use piecewise tube grading in material properties, wall thickness, and length to develop lighter composite tube designs with improved dynamic stability and increased flutter speed.

Oke and Khulief [21] used a finite element formulation based on B-spline wavelets on an interval to model composite tube-free vibrations. Wavelet space is used to construct the finite tube first, and then it is transported to the physical space. Analytically Wavelet functions and B-splines can represent composite tube mass and stiffness matrices. There is also a consideration of the Euler-Bernoulli beam theory and the Timoshenko beam theory. The

modal characteristics of the composite tube may be calculated using an extended eigenvalue problem. Compared to the traditional finite element method, the suggested wavelet-based discretization methodology for composite tube modeling employs a fraction of the components.

Khudayarov et al.[22] investigated the Vibration problems of pipelines made of composite materials with account for lumped masses. A mathematical model of the motion of pipelines conveying fluid flow is developed based on the Winkler base with account for viscosity properties of the material of structures and pipeline bases, axial forces, internal pressure, resistance forces, and lumped masses. The Boltzmann-Volterra integral model with weakly singular hereditary kernels describes viscoelastic material strain processes. Using the Bubnov-Galerkin method, the problem is reduced to studying a system of ordinary integro-differential equations. A computational algorithm is developed to eliminate the features of integral-differential equations with weakly singular kernels, followed by quadrature formulas. The effect of rheological parameters of the pipeline material, lumped masses, internal pressure, Reynolds numbers, and base parameters on the vibration of a viscoelastic pipeline conveying fluid flow are analyzed. It is revealed that the viscosity parameters of the material and the pipeline base lead to a significant change in critical flow rate. It was found that an increase in the viscosity parameter, the parameters of lumped masses, and internal pressure leads to a decrease in critical flow rate. It is shown that when the lumped masses are moved away from the center along the pipeline length, the vibration frequency increases.

2.2.3 Tube conveying fluid with the effect of Internal damping

Internal damping is a critical design parameter of dissipation energy in materials under stress, particularly for vibrating structures used in the oil and car industries. Damping in various engineering metals has been explored using various experimental and computational approaches. Furthermore, because damping varies with several environmental conditions, many distinct parameters were employed in those investigations.

Patel [23] An internally damped tapered truncated cantilever beam was investigated for vibrations. There are two viable solutions for a square cross-section beam with linear depth and breadth variation: (1) a discrete mass distribution and (2) a continuous mass distribution. The beam should be viscoelastic at Kelvin temperatures. Precision oscillation frequency, mode shape, and steady-state response solutions may be found in this topic. The results of discrete and continuous experiments employing the first two modes of a typical beam were compared. The natural frequencies of the two approaches are just around 9% different, and the mode shapes are nearly identical. The beam's steady-state response to harmonic stimulation is calculated. The response of the discrete model is calculated using the excitation frequency as the fundamental natural frequency of the beam. Because assessing Bessel functions with intricate data is difficult, continuous analysis cannot respond.

Kroisová [24] investigated the damping properties of epoxy composite materials. Composite structures were built utilizing a two-component of epoxy resin and a variety of fillers to perform testing (lead particles and chippings, ferrous - ferric oxide particles, titanium dioxide particles, alloy hollow tubes, carbon chopped fibers, and cork particles). The fillers in the

polymer matrix varied in composition, particle size, shape, and weight percentage. Damping tests on the cast and cured epoxy composite systems were carried out at a temperature of 220 C, a low frequency of 50 Hz to 100 Hz, and atmospheric pressure, representing the structure's dynamic stress condition. The deflection of samples was measured using photoelectric equipment, and the loss coefficient was determined using a traditional method. The form, size, surface of the fillers, fracture surfaces, and interfaces of composites were all studied using SEM microscopy.

Wang et al. [25] studied the dynamics of supported fluid-conveying tubes with geometric imperfections by considering the integral–partial–differential equation of motion. The effect of sinusoidal wave or parabolic variations of imperfections is investigated for the system's four-degree-of-freedom ($N^{1/4}$) model. Linear analysis shows that each type of imperfection affects the natural frequency of only one single mode. For half-sinusoidal wave or parabolic variation of imperfections, the critical flow velocity at which buckling instability occurs is higher than for a tube without imperfections. The tube remains in its undeformed static equilibrium state at low flow velocity in all cases. At high flow velocity, however, the nonlinear analysis predicts that the tube would be attracted to one of two other nontrivial equilibria, which, more importantly, maybe asymmetric due to the presence of imperfections. For tubes with imperfection in the form of half-sinusoidal wave or parabolic variation, interestingly, the nonlinear theory predicts that a small buckling displacement would occur at flow velocities slightly lower than the critical flow velocity predicted by the linear theory.

Colakoglu [26] found that The internal damping of metallic materials varies with many different environmental effects. These are the frequency,

amplitude of strain or stress, and temperature. In addition, internal damping is affected by corrosion fatigue, grain size, and porosity. The damping also depends on the number of fatigue cycles. There is a functional relationship between the damping, number of cycles, and applied stress. These seven different environmental factors and their effects on the damping are analyzed in the case of 6061 aluminum alloy. The relationships between the damping and every effective factor vary depending on the aluminum type.

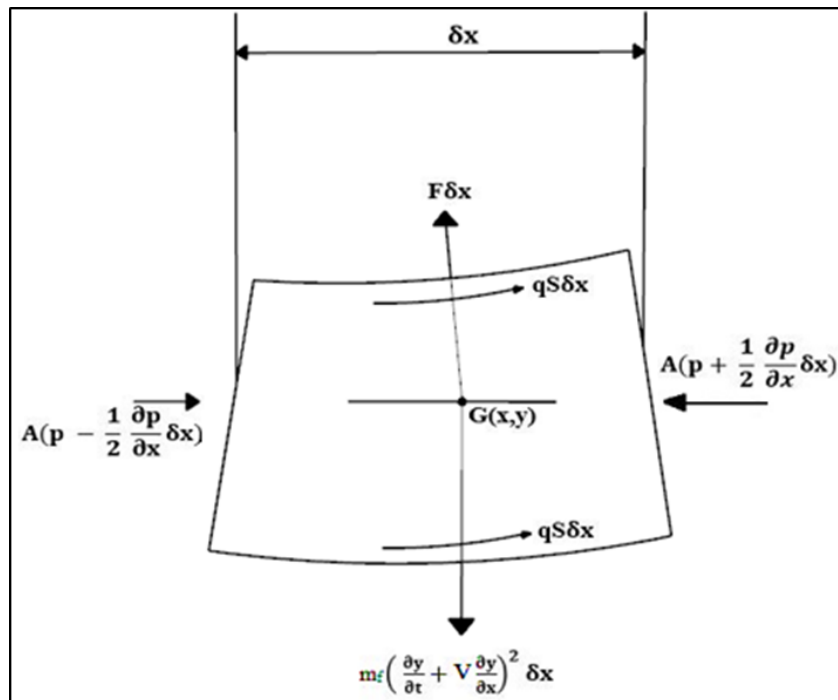
Karic et al. [27] presented results from estimating internal structural damping coefficients for bending free vibrations of elastic systems. The internal damping force created by the deformation of a structure is supposed to be proportional to velocity. The New-Mark method was utilized to obtain the vibrating structure's temporal response. The computational coefficient of internal damping was modified on elastic cantilever beams to match the experimental results. As a result, there is a strong correlation between the cross-sectional moment of inertia and the damping factor. The correlations fit the structural damping hypothesis.

2.3 Summary

Previous studies found that little research focused on the dynamics of tubes made of composite materials that convey fluid, especially from the analytical point of view. Therefore, the current research is directed to this point in addition to determining the effect of internal damping on the natural frequency of the tube. Also, an analytical approach will be made to derive the equation of motion for tubes made of composite materials that convey fluids at different flow velocities. In order to demonstrate the effectiveness of the analytical solution, a simple device is manufactured.



Mathematical Modeling



Chapter Three

Mathematical Modelling

3.1 Introduction

This chapter covers the theoretical analysis of the dynamics of a straight tube conveying internal flowing fluid. The tube is considered a single-span tube and multi-span tube supported by clamped and simple supports. The derivation of the equation of motion is done by using Newton's second law. The fluid flow is assumed to be steady, and the effective parameters will be taken into account in deriving the equation of motion of tube - fluid system.

3.2 Materials and Methods

This work studies the dynamics of a composite tube conveying a steady flow. The derivation of the governing equation is based on the Euler-Bernoulli theorem. The following assumptions are considered to simplify the complexities of the derivation, which have negligible effects:

- 1- Neglecting the influence of gravity by assuming horizontal tube.
- 2- The tube is inextensible.
- 3- Neglecting the effect of rotary inertia and shear deformation.
- 4- Small tube lateral motion.
- 5- Neglecting the details of fluid flow, such as the flow velocity distribution across tube sections.

Before balancing forces and moments, it is essential to explain the velocity and acceleration of the fluid element that moves axially inside the tube and laterally with the vibrational motion of the tube. The velocity of the fluid element is composed of two components; the first is the axial flow velocity V and the second is the lateral velocity of the fluid due to the vibrational motion $\frac{\partial y}{\partial t}$ Where y is the lateral motion of the tube.

Expressing the equation for the lateral velocity of the fluid element [28]: -

$$V_f = \frac{\partial y}{\partial t} + V \frac{\partial y}{\partial x} \quad (3.1)$$

The acceleration of the fluid element is the resultant of the components as given by the following equation [10]:-

$$a_f = \frac{\partial V_f}{\partial t} = \frac{\partial^2 y}{\partial t^2} + 2V \frac{\partial^2 y}{\partial y \partial t} + V^2 \frac{\partial^2 y}{\partial x^2} + \frac{\partial V}{\partial t} \frac{\partial y}{\partial x} \quad (3.2)$$

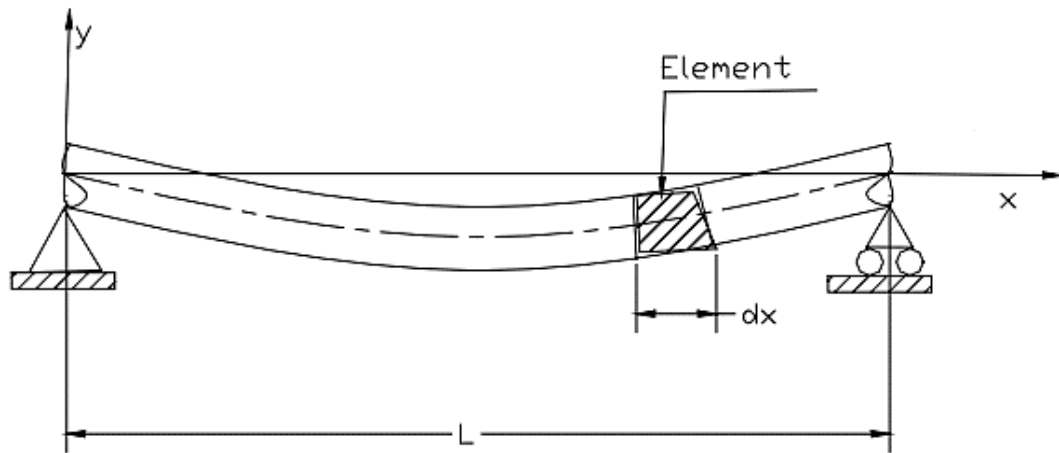


Figure (3.1). A fluid-conveying tube with simply supported ends

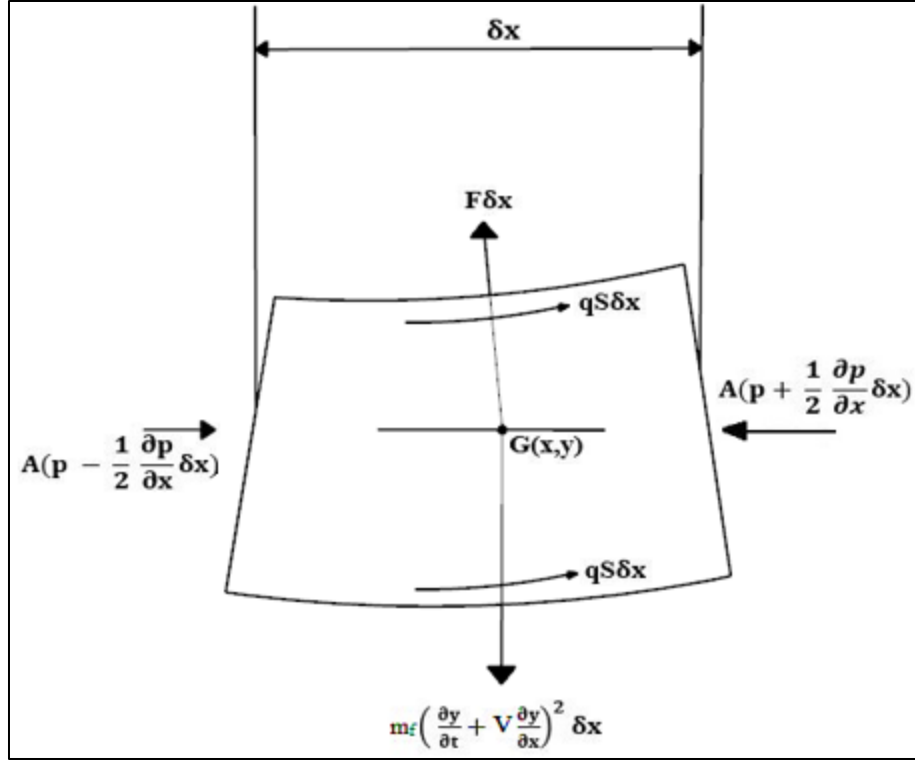


Figure (3.2). Representation of forces acting on the fluid element.

Balancing axial forces along the x-axis on the fluid element, shown in figure (3.2), results in the following equation. [10]

$$-A \frac{\partial p}{\partial x} - q S + F \frac{\partial y}{\partial x} = 0 \quad (3.3)$$

The force balance in the lateral direction, along the y-axis, yields [29]

$$F + A \frac{\partial}{\partial x} \left(P \frac{\partial y}{\partial x} \right) + m_f \left(\frac{\partial y}{\partial t} + V \frac{\partial y}{\partial x} \right)^2 = 0 \quad (3.4)$$

Where F denotes the transverse force per unit length between the tube wall and the fluid, and S denotes the tube's internal perimeter.

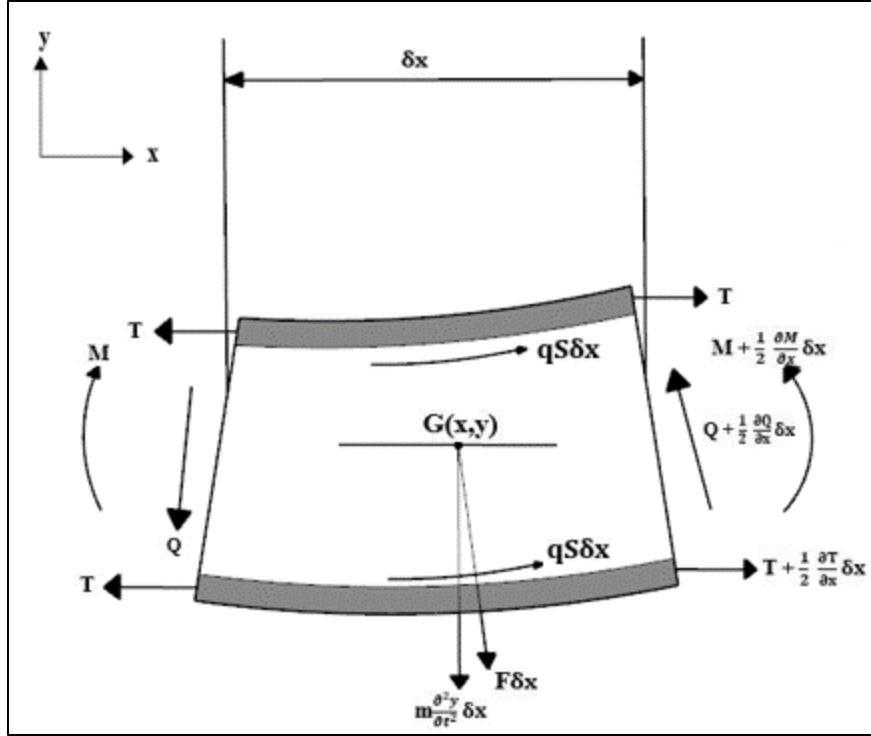


Figure (3.3). Representation of forces acting on the tube element.

The balancing of forces on the tube element in the axial direction along the x-axis is shown in figure (3.3) [4];

$$\frac{\partial T}{\partial x} + q S - F \frac{\partial y}{\partial x} = 0 \quad (3.5)$$

Force balance in the y-direction is [28];

$$\frac{\partial Q}{\partial x} + \frac{\partial}{\partial x} \left(T \frac{\partial y}{\partial x} \right) + F - m_t \frac{\partial^2 y}{\partial t^2} = 0 \quad (3.6)$$

According to the tube deformation, the transverse shear force Q in the tube is related to the bending moment M by [29]:

$$\frac{\partial M}{\partial x} + Q = 0 \quad \gg \quad Q = - \frac{\partial M}{\partial x} \quad (3.7)$$

The equation of bending moment (M) is [22]: -

$$M = E I \frac{\partial^2 y}{\partial x^2} + E^* I \frac{\partial^3 y}{\partial x^2 \partial t} \quad (3.8)$$

Substituting Eq. (3.8) into Eq. (3.7) makes the transverse shear force Q in the tube be written as [5]:

$$Q = - (E^* \frac{\partial}{\partial t} + E) I \frac{\partial^3 y}{\partial x^3} \quad (3.9)$$

Where, E^* Is the internal damping coefficient [25].

$$\frac{\partial}{\partial x} (T - PA) = 0 \quad (3.10)$$

Integrating the above equation yields [10]

$$(T - PA) = C \quad (3.11)$$

Where C is a constant.

At the end of the tube where $x=L$, the tension value is zero $T=0$ and $P = P_i$, substituting that into Eq. (3.11) gives [28]

$$T - PA = - P_i A \quad (3.12)$$

Combining equations (3.4), (3.6), and (3.9) results in the following partial differential equation [25]:

$$\begin{aligned} \frac{\partial}{\partial x} \left((E^* \frac{\partial}{\partial t} + E) I \frac{\partial^3 y}{\partial x^3} \right) + \frac{\partial}{\partial x} \left[(T - PA) \frac{\partial y}{\partial x} \right] \\ - m_f \left(\frac{\partial y}{\partial t} + V \frac{\partial y}{\partial x} \right)^2 - m_t \frac{\partial^2 y}{\partial t^2} = 0 \end{aligned} \quad (3.13)$$

Substituting Eq. (3.12) into Eq. (3.13) to get the equation of motion of a tube conveying fluid taking into account the effect of the internal damping coefficient, which is [25]

$$\begin{aligned} E^* I \frac{\partial^5 y}{\partial x^4 \partial t} + E I \frac{\partial^4 y}{\partial x^4} - [(m_f V^2 + P_i A)] \frac{\partial^2 y}{\partial x^2} \\ + 2 m_f V \frac{\partial^2 y}{\partial x \partial t} + m_f \frac{\partial V}{\partial t} \frac{\partial y}{\partial x} + (m_f + m_t) \frac{\partial^2 y}{\partial t^2} = 0 \end{aligned} \quad (3.14)$$

Modulus of elasticity of composite material of the tube can be written according to the Rule of Mixtures, as follows [30]

$$E_c = E_F V_F + E_M V_M \quad (3.15)$$

$$(V_M + V_F) = 1 \quad (3.16)$$

By knowing the volume fraction of the fiber, the elastic modulus is written as [30]

$$E_c = E_F V_F + E_M (1 - V_F) \quad (3.17)$$

Where, $E_c = E_{eq}$ For multi-layer of the composite tube conveying fluid .

Substituting E_{eq} into Eq. (3.14) with neglecting the term $(\frac{\partial V}{\partial t})$ because the flow is assumed to be steady, the equation of motion of the composite tube conveying fluid with the effect of internal damping is written as;

$$\begin{aligned} E^*_{eq} I \frac{\partial^5 y}{\partial x^4 \partial t} + E_{eq} I \frac{\partial^4 y}{\partial x^4} - [(m_f V^2 + P_i A)] \frac{\partial^2 y}{\partial x^2} \\ + 2 m_f V \frac{\partial^2 y}{\partial x \partial t} + (m_f + m_t) \frac{\partial^2 y}{\partial t^2} = 0 \end{aligned} \quad (3.18)$$

Equation (3.18) is in a dimensional form. For generality, it is more convenient to write this equation in a dimensionless form by using the following nondimensional notations;

$$\text{where: } \eta = \frac{y}{L} , \quad \xi = \frac{x}{L} , \quad U = VL \sqrt{\frac{m_f}{EI}} , \quad \gamma = \frac{P_i A L^2}{EI}$$

$$\tau = \frac{t}{L^2} \sqrt{\frac{EI}{m_f+m_p}} \quad \text{and} \quad \beta = \sqrt{\frac{m_f}{m_f+m_p}}$$

Use the above dimensionless groups with equation (3.18) to get [28]:

$$\mu \dot{\eta}^{IV} + \eta^{IV} + (U^2 + \gamma)\eta'' + 2\beta U \dot{\eta}' + \ddot{\eta} = 0 \quad (3.19)$$

$$\text{Where } \eta^I = \frac{\partial^I \eta}{\partial \xi^I} \quad \text{and} \quad \dot{\eta} = \frac{\partial \eta}{\partial \tau}$$

3.3 Vibration Analysis

This section will evaluate the natural frequencies and the vibration characteristics of tubes conveying fluid.

The solution of this equation is composed of the following spatial time variables, [10]:

$$\eta(\xi, \tau) = \sum_{j=1}^4 c_j e^{i\lambda_j \xi} e^{i\Omega \tau} \quad (3.20)$$

Substituting Eq. (3.20) into Eq. (3.19) results in a fourth-order polynomial equation for λ as follows :

$$\mu \Omega \lambda^4 + \lambda^4 - (U^2 + \gamma) \lambda^2 - 2\beta U \Omega \lambda - \Omega^2 = 0 \quad (3.21)$$

Where Ω is the dimensionless circular frequency of oscillation which is [29]:

$$\Omega = \omega L^2 \sqrt{\frac{(m_f + m_p)}{EI}}$$

Where ω is the circular natural frequency (rad/sec)

Substituting the roots resulting from the polynomial (3.21) into Eq. (3.20) and using the boundary conditions, the natural frequency can be calculated.

3.3.1 Boundary conditions

The following boundary conditions are considered to support the tube under investigation.

1- Simply supported

When the tube is simply supported at its ends, both the lateral displacement and bending moment are zero. These two conditions are satisfied mathematically as [10];

$$\left\{ \begin{array}{l} \text{At } x = 0 \quad ; \quad \eta(0, \tau) = 0, \eta''(0, \tau) = 0 \\ \text{At } x = L \quad ; \quad \eta(L, \tau) = 0, \eta''(L, \tau) = 0 \end{array} \right\} \quad (3.22)$$

By solving the problem with the government equation (3.21) which the same solve for all supported.

$$\eta(\xi, \tau) = \sum_{j=1}^4 c_j e^{i\lambda_j \xi} e^{i\Omega \tau}$$

$$\eta(0, \tau) = [c_1 + c_2 + c_3 + c_4]$$

$$\eta(1, \tau) = [c_1 + c_2 + c_3 + c_4][(\cos(\lambda_R) - \sin(\lambda_R)) e^{-\lambda_J}]$$

$$\eta''(\xi, \tau) = -\lambda_j^2 \sum_{j=1}^4 c_j e^{i\lambda_j \xi} e^{i\Omega \tau}$$

$$\eta''(0, \tau) = [c_1 + c_2 + c_3 + c_4][\lambda_R^2 + 2i\lambda_R \lambda_J - \lambda_J^2]$$

$$\eta''(1, \tau) = [c_1 + c_2 + c_3 + c_4][\lambda_R^2 + 2i\lambda_R \lambda_J - \lambda_J^2][(\cos(\lambda_R) - \sin(\lambda_R)) e^{-\lambda_J}]$$

2- Clamped support

For clamped end conditions, each of the lateral displacement and slope is zero and can be represented as [10];

$$\left\{ \begin{array}{l} \text{At } x = 0 \quad ; \eta(0, \tau) = 0 \quad , \quad \eta'(0, \tau) = 0 \\ \text{At } x = L \quad ; \eta(L, \tau) = 0 \quad , \quad \eta'(L, \tau) = 0 \end{array} \right\} \quad (3.23)$$

3- Intermediate support

If simple support is imposed in the middle between two clamped spans, each span has a length of L. The conditions are;

$$\left\{ \begin{array}{l} \text{At } x = 0 \quad , \quad \eta(0, \tau) = 0, \quad \eta'(0, \tau) = 0 \\ \text{At } x = L \quad , \quad \eta(L, \tau) = 0 \quad , \quad \eta'(L, \tau) = \eta'(0, \tau) \\ \quad \quad \quad \eta''(L, \tau) = \eta''(0, \tau) \quad , \quad \eta(0, \tau) = 0 \\ \text{At } x = L \quad , \quad \eta(L, \tau) = 0, \quad \eta'(L, \tau) = 0 \end{array} \right\} \quad (3.24)$$

4- Clamped - pinned support

For Clamped - pinned end conditions, each of the lateral displacement, slope, and bending moments is zero, which can be represented as [10];

$$\left\{ \begin{array}{l} \text{At } x = 0 \quad ; \quad \eta(0, \tau) = 0 \quad , \quad \eta'(0, \tau) = 0 \\ \text{At } x = L \quad ; \quad \eta(L, \tau) = 0 \quad , \quad \eta''(L, \tau) = 0 \end{array} \right\} \quad (3.25)$$

5- Clamped -free support

For Clamped – free end conditions, each of the lateral displacement, slope, bending moment, and shear force is zero, which can be represented as [17];

$$\left\{ \begin{array}{l} \text{At } x = 0 \quad ; \quad \eta(0, \tau) = 0 \quad , \quad \eta'(0, \tau) = 0 \\ \text{At } x = L \quad ; \quad \eta''(L, \tau) = 0 \quad , \quad \eta'''(L, \tau) = 0 \end{array} \right\} \quad (3.26)$$

6- Free - free support

For free–free end conditions, each of the bending moment and shear force is zero, which can be represented as;

$$\left\{ \begin{array}{l} \text{At } x = 0 \quad ; \quad \eta''(0, \tau) = 0 \quad , \quad \eta'''(0, \tau) = 0 \\ \text{At } x = L \quad ; \quad \eta''(L, \tau) = 0 \quad , \quad \eta'''(L, \tau) = 0 \end{array} \right\} \quad (3.27)$$

3.3.2 Tube Natural Frequencies

The natural frequency of the tube can be calculated by substituting the solution given by Eq. (3.21) in the corresponding boundary conditions. This substitution results in a set of coupled equations written in a matrix form. The form of the matrix, the values of the matrix elements, depending on the type of the boundary conditions used. In a tube simply supported at both ends, where the displacements and bending moments are zero, all matrix elements depend on the boundary condition. The matrix equation is written as [10];

$$\begin{bmatrix} 1 & 1 & 1 & 1 \\ \lambda^2 & \lambda^2 & \lambda^2 & \lambda^2 \\ e^\lambda & e^\lambda & e^\lambda & e^\lambda \\ \lambda^2 e^\lambda & \lambda^2 e^\lambda & \lambda^2 e^\lambda & \lambda^2 e^\lambda \end{bmatrix} \begin{Bmatrix} C_1 \\ C_2 \\ C_3 \\ C_4 \end{Bmatrix} = \begin{Bmatrix} 0 \\ 0 \\ 0 \\ 0 \end{Bmatrix} \quad (3.28)$$

When the tube is clamped at both ends, the zero values of both the displacement and slope at both ends make the matrix equation be written as :

$$\begin{bmatrix} 1 & 1 & 1 & 1 \\ \lambda & \lambda & \lambda & \lambda \\ e^\lambda & e^\lambda & e^\lambda & e^\lambda \\ \lambda e^\lambda & \lambda e^\lambda & \lambda e^\lambda & \lambda e^\lambda \end{bmatrix} \begin{Bmatrix} C_1 \\ C_2 \\ C_3 \\ C_4 \end{Bmatrix} = \begin{Bmatrix} 0 \\ 0 \\ 0 \\ 0 \end{Bmatrix} \quad (3.29)$$

If the tube is clamped at one end and simply supported at the other, the matrix will be composed of the elements related to the clamped end, and those of the simply supported one, and it is written as:

$$\begin{bmatrix} 1 & 1 & 1 & 1 \\ \lambda & \lambda & \lambda & \lambda \\ e^\lambda & e^\lambda & e^\lambda & e^\lambda \\ \lambda^2 e^\lambda & \lambda^2 e^\lambda & \lambda^2 e^\lambda & \lambda^2 e^\lambda \end{bmatrix} \begin{Bmatrix} C_1 \\ C_2 \\ C_3 \\ C_4 \end{Bmatrix} = \begin{Bmatrix} 0 \\ 0 \\ 0 \\ 0 \end{Bmatrix} \quad (3.30)$$

When the tube is supported by more than two supports, one at each end and another at the mid-span, the matrix will be doubled. In the case of a tube clamped at the extreme ends and simply supported at the middle, the matrix equation is written as:

$$\begin{bmatrix} 1 & 1 & 1 & 1 & 0 & 0 & 0 & 0 \\ \lambda & \lambda & \lambda & \lambda & 0 & 0 & 0 & 0 \\ e^\lambda & e^\lambda & e^\lambda & e^\lambda & 0 & 0 & 0 & 0 \\ \lambda e^\lambda & \lambda e^\lambda & \lambda e^\lambda & \lambda e^\lambda & \lambda & \lambda & \lambda & \lambda \\ \lambda^2 e^\lambda & \lambda^2 e^\lambda & \lambda^2 e^\lambda & \lambda^2 e^\lambda & \lambda^2 & \lambda^2 & \lambda^2 & \lambda^2 \\ 0 & 0 & 0 & 0 & 1 & 1 & 1 & 1 \\ 0 & 0 & 0 & 0 & e^\lambda & e^\lambda & e^\lambda & e^\lambda \\ 0 & 0 & 0 & 0 & \lambda e^\lambda & \lambda e^\lambda & \lambda e^\lambda & \lambda e^\lambda \end{bmatrix} \begin{Bmatrix} C_1 \\ C_2 \\ C_3 \\ C_4 \\ C_5 \\ C_6 \\ C_7 \\ C_8 \end{Bmatrix} = \begin{Bmatrix} 0 \\ 0 \\ 0 \\ 0 \\ 0 \\ 0 \\ 0 \\ 0 \end{Bmatrix} \quad (3.31)$$

If the tube is clamped at one end and free at the other, where the lateral displacement, slope, bending moment, and shear force are zero, the resulted matrix equation is:

$$\begin{bmatrix} 1 & 1 & 1 & 1 \\ \lambda & \lambda & \lambda & \lambda \\ \lambda^2 e^\lambda & \lambda^2 e^\lambda & \lambda^2 e^\lambda & \lambda^2 e^\lambda \\ \lambda^3 e^\lambda & \lambda^3 e^\lambda & \lambda^3 e^\lambda & \lambda^3 e^\lambda \end{bmatrix} \begin{Bmatrix} C_1 \\ C_2 \\ C_3 \\ C_4 \end{Bmatrix} = \begin{Bmatrix} 0 \\ 0 \\ 0 \\ 0 \end{Bmatrix} \quad (3.32)$$

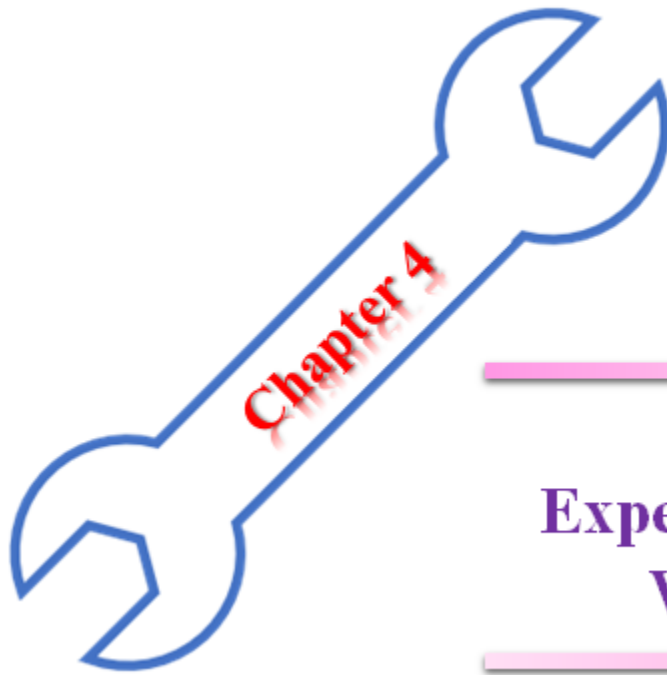
When the tube is free at both ends, the bending moment and shear force are zero; the matrix equation will be written as:

$$\begin{bmatrix} \lambda^2 & \lambda^2 & \lambda^2 & \lambda^2 \\ \lambda^3 & \lambda^3 & \lambda^3 & \lambda^3 \\ \lambda^2 e^\lambda & \lambda^2 e^\lambda & \lambda^2 e^\lambda & \lambda^2 e^\lambda \\ \lambda^3 e^\lambda & \lambda^3 e^\lambda & \lambda^3 e^\lambda & \lambda^3 e^\lambda \end{bmatrix} \begin{Bmatrix} C_1 \\ C_2 \\ C_3 \\ C_4 \end{Bmatrix} = \begin{Bmatrix} 0 \\ 0 \\ 0 \\ 0 \end{Bmatrix} \quad (3.33)$$

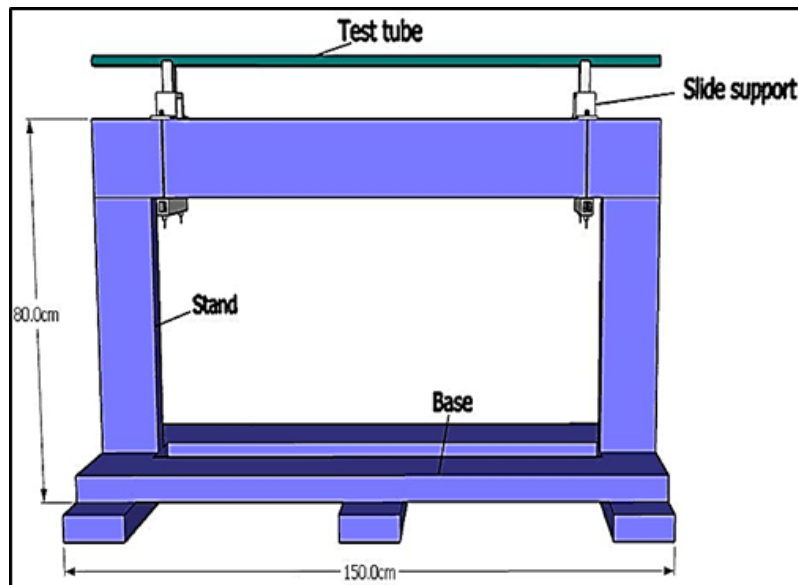
To solve the simply supported and another ends, substituting Eq. (3.20) into boundary condition, the results matrix equation :

$$\begin{bmatrix} a_{11} & a_{12} & a_{13} & a_{14} \\ a_{21} & a_{22} & a_{23} & a_{24} \\ a_{31} & a_{32} & a_{33} & a_{34} \\ a_{41} & a_{42} & a_{43} & a_{44} \end{bmatrix} \begin{Bmatrix} c_1 \\ c_2 \\ c_3 \\ c_4 \end{Bmatrix} = \begin{Bmatrix} 0 \\ 0 \\ 0 \\ 0 \end{Bmatrix} \quad (3.34)$$

The steps of calculation are shown in Appendix A.



Experimental Work



Chapter Four

Experimental Work

4.1 Introduction

This chapter deals with the experimental work to validate the theoretical analysis presented in the previous chapter. The natural frequency of the tube under investigation is measured experimentally with the available boundary conditions. Water is used as the flowing fluid in the tube via a water pump, and a flowmeter is used to measure the flow rate value. Different values of flow velocities of the fluid are considered to show the effect of flow velocity on the free vibration of the tube. A DC motor is used to excite the tube laterally to distinguish the tube's natural frequency.

4.2 Testing models

The present work used three types of composite tubes with the properties shown in Table (4.1).

Table (4.1). Specifications of tested models.

No. of Model	D_o (m)	D_i (m)	t(m)	m (kg) of L= 0.02m
1	0.023	0.013	0.005	0.012
2	0.015	0.007	0.004	0.007
3	0.013	0.007	0.003	0.003

4.3 Test Rig

A suitable apparatus has been manufactured to implement the required tests. The apparatus is composed of the following components;

- 1- The basic structure of the apparatus represents the base to the other components and welded steel members connected. This structure includes the tube supports, as shown in figures (4.1,4.2).
- 2- The tested tube.
- 3- Exciting motor.
- 4- Flowmeter.
- 5- Water pump.
- 6- Reservoir (Water tank)

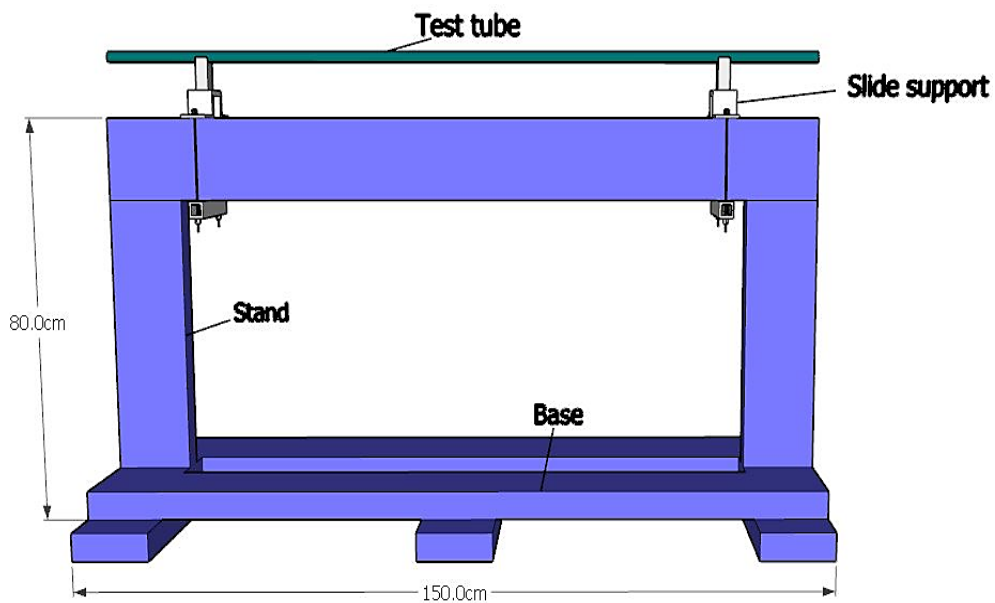


Figure (4.1). Schematic diagram of the basic structure.

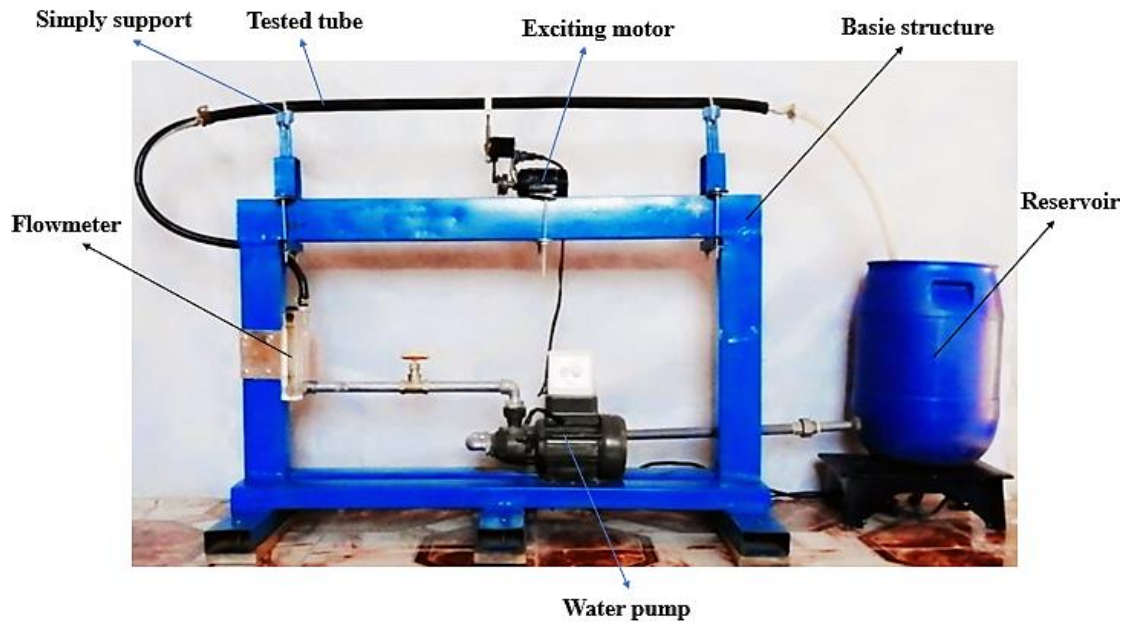


Figure (4.2). The structure and the different parts of the test rig.

Components 4, 5, and 6 represent the water circuit which is represented by the schematic diagram shown in figure (4.3)

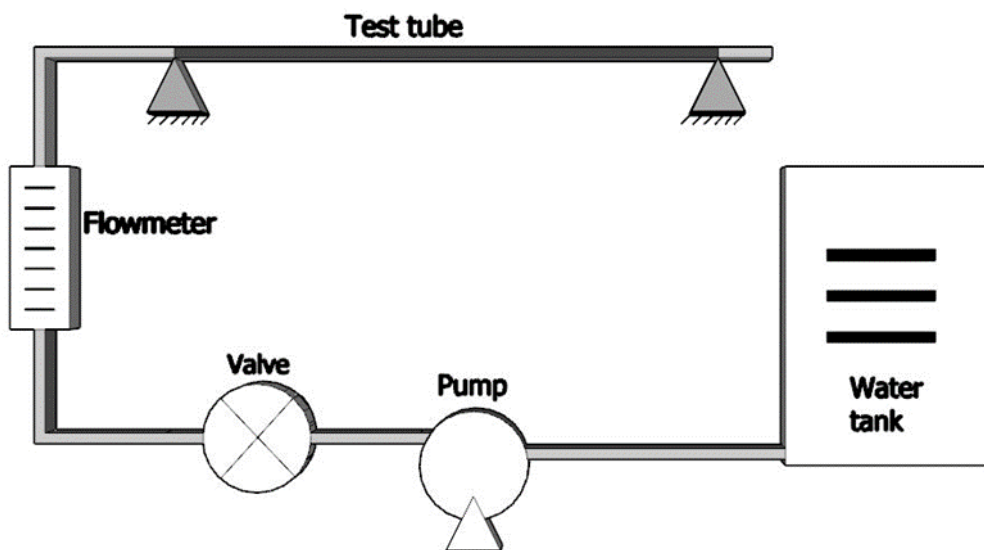


Figure (4.3). Schematic diagram of the circle of water.

4.4 Vibration test

The mechanisms shown in figure (4.4) was used to excite the tested tube laterally via a DC electric motor with a crankshaft

A voltage regulator controls the motor speed to get the required speed. The crankshaft was used to produce a controlled harmonic motion.

The function of the connecting arm mechanism was transferring the harmonic motion from the crankshaft to the knocking shaft to excite the tested tube.

The mechanism is to change the rotational speed of the crankshaft and thus rotate the knocking shaft by the connecting arm to excite the tested tube. The DC motor speed is measured by digital laser tachometer type (DT-2234), as shown in figure (4.5).

The principle of working of this device is installing a silver-colored adhesive piece placed on the spindle of the crankshaft and then directing the laser beam of the tachometer device on the axis of rotation, whereby changing the speed of rotation by the regulator, the crankshaft moves at different speeds. This leads to the rotation of the sticker to cut the laser beam with each lap of rotation during one minute so that the number of laps is displayed on the digital screen of the tachometer. Thus, the rotational speed of the crankshaft is measured.

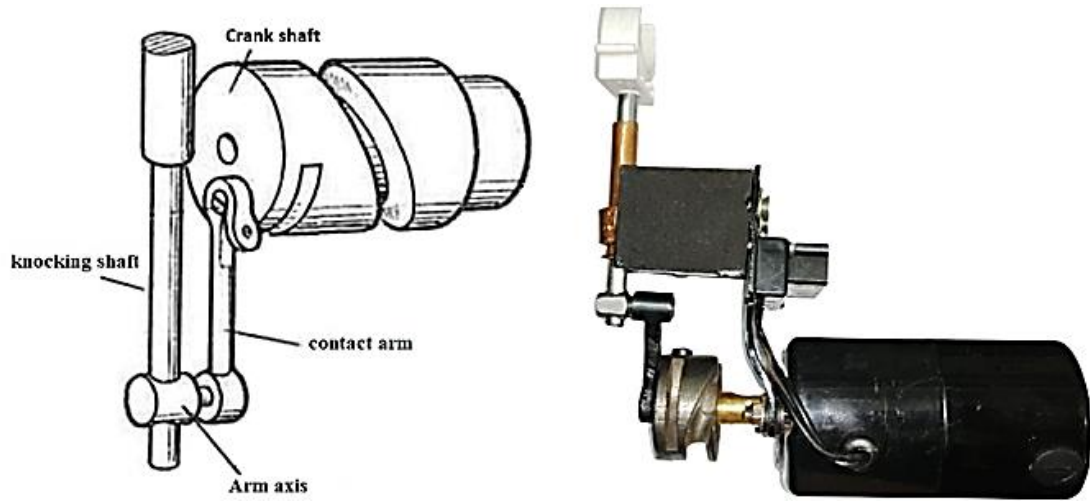


Figure (4.4). Vibration generator parts.



Figure (4.5). Digital laser RPM Tachometer.

4.5 Modulus of Elasticity and Density of the tube

The tested tubes are all composed of the same material, carbon-fiber epoxy, but their internal and external diameters varied. The modulus of elasticity of the tube is estimated by applying a load at the mid-span of a simply supported tube of a 12 cm length and measuring the amount of deflection. The load-deflection is shown in figure (4.6). The modulus of elasticity for all tubes used in the test was 2.6 Gpa, which was calculated by the following equation:

$$E = \frac{L^3}{48 I M_{1-d}} \quad , \text{ where } M_{1-d} = \frac{\text{deflection}}{\text{load}}$$

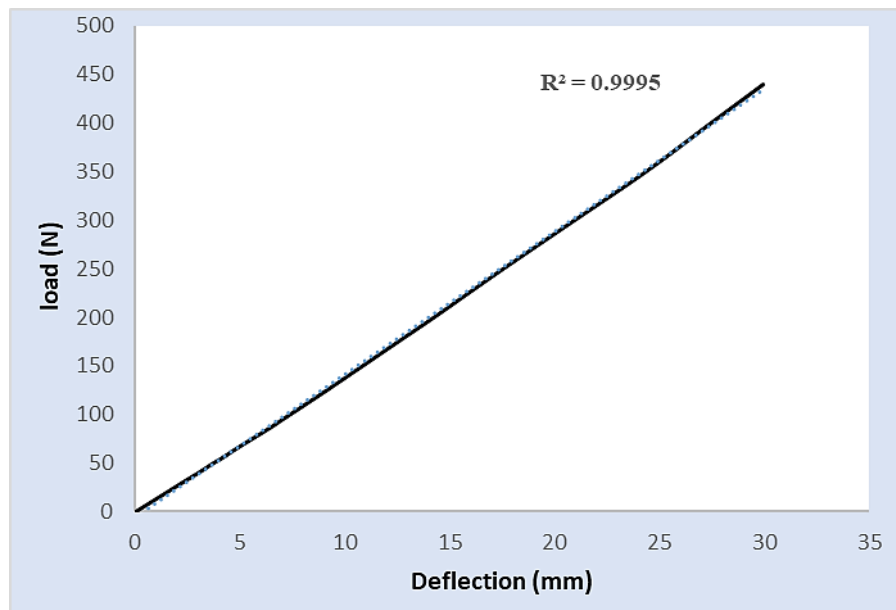


Figure (4.6). Load–deflection curve of a simply supported composite tube.

The density is estimated by taking a 2 cm length of each tube, and the mass is measured by an electronic low-scale that reads three decimal digits. The density for all tubes of $L= 0.02\text{m}$ used in the test was 2122.091 Kg/m^3 . The following formula was used to determine the density of the test tubes :

$$\rho_t = \frac{4 m}{\pi L (D_o^2 - D_i^2)} \quad (4.1)$$

Where m is mass of tube, D_o and D_i are the outside and inner diameters of the test tube, respectively.

4.6 Calibration of Flowmeter

The flowmeter is calibrated by collecting 20 liters and measuring the time required to collect this volume of water. This process is repeated three times, and the average time value is calculated to minimize the error. The flowmeter and tank volume calibration curve is shown in figure (4.7).

The velocity of the fluid passing through the test tube can be determined by measuring the flow rate using the following relationship:

$$Q (\text{m}^3/\text{s}) = V (\text{m/s}) * A (\text{m}^2) \quad (4.2)$$

Where; Q is the fluid flow rate, V is the fluid flow velocity, and A is the internal cross-section area.

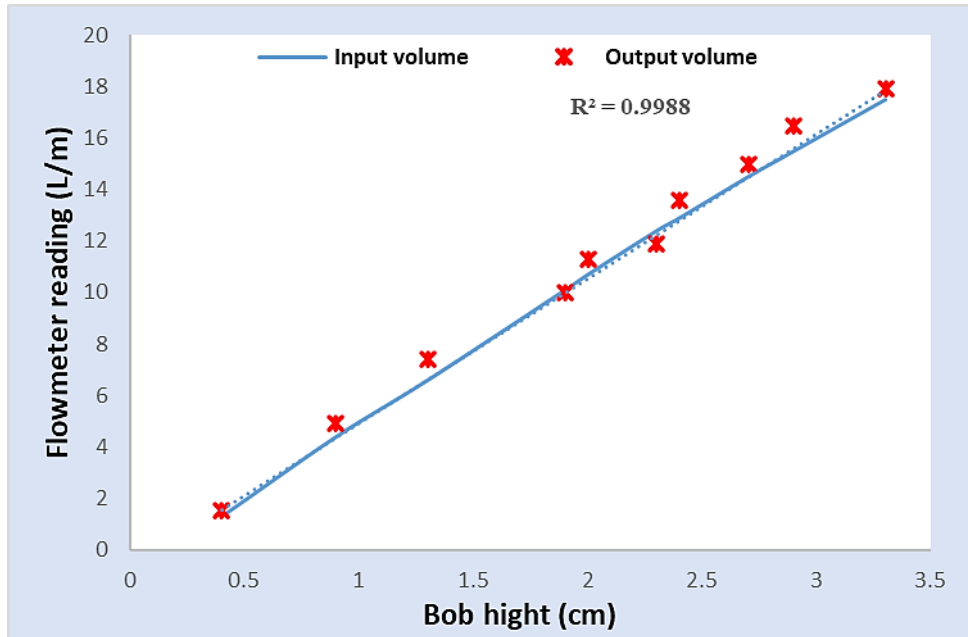
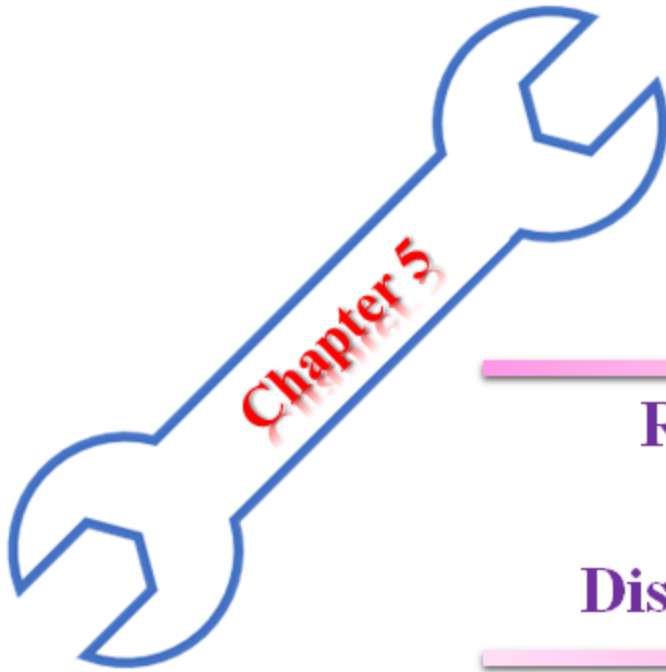


Figure (4.7). The curve of calibration for a flowmeter.

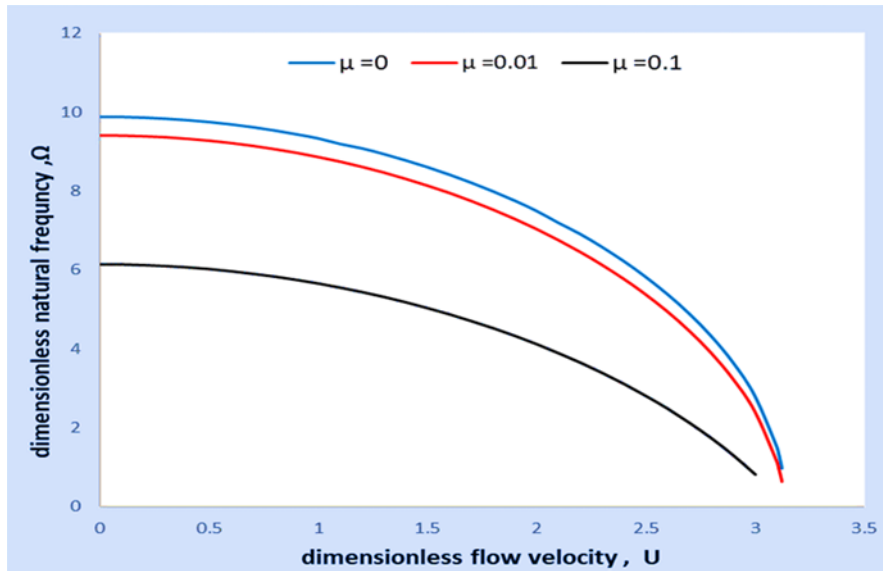
4.7 Experimental Natural Frequency Test

This test includes three boundary conditions for the carbon fiber tube: simply supported, firmly supported, and bolted support. For all models, the tube length is 0.82 m, and the maximum flow rate is 20 l/min.

A crankshaft mechanism connected to the regulator, a speed controller, excited the tube. The engine speed gradually increases until the resonance appears. The rotational speed of the crankshaft is then recorded using the number of turns displayed on the tachometer's digital display. Convert tachometer units from RPM to Rad/sec to find ω_n .



Result & Discussion



Chapter Five

Results and Discussion

5.1 Introduction

The theoretical and experimental findings related to the tubes made of composite material conveying fluid are provided in this chapter. The effects of flow velocity, internal damping, and type of boundary conditions on the dynamics of the tube were calculated and presented through tables and graphs. The experimental results were compared with the theoretical results to find the error ratio.

5.2 Theoretical Results

Theoretical results deal with the variation of the natural frequency of a composite tube affected by main parameters. This is done by solving the governing equation, represented by Eq. (3.21), for selected boundary conditions. Some of the present results were compared with other published works for verification. The theoretical results include the following:

5.2.1 Effect of flow velocity on the natural frequency

The first step in evaluating the results in this work is represented by calculating the first two modes of free vibration of the composite material tube by using the governing equation and assuming flow velocity is zero for different boundary conditions as shown in table (5.1).

The results show that the tube with zero flow has the same natural frequency as that for a beam with the same specifications and type of end support. This conclusion is significant where it indicates that the results presented here are on the right side.

Table (5.1). The first two modes natural frequencies of the composite tube with different types of supporting, $U = 0$, $\gamma = 0$, and $\beta = 0.6336$ [31].

No.	Beam Configuration	First mode	Second mode
1	Simply support	9.872	39.5
2	Clamped support	22.376	61.7
3	Clamped-pinned support	15.424	50.0
4	Clamped-free support	3.521	22.0
5	Free-free support	22.375	61.7

The variations of the first and second dimensionless natural frequencies with a dimensionless flow velocity of the composite tube for each type of support are presented in figures (5.1 to 5.6). The results presented in these figures are taken for $\gamma=0$, $\beta=0.6336$, and $\mu=0$.

From these figures, one can get the following results;

1. The natural frequency decreased with the gradual increase in the flow velocity until it reached almost zero, which means that the tube lost its stability due to the buckling phenomenon. The value of the flow velocity of the fluid at which the natural frequency approaches zero is called the "critical flow velocity". This means that the fluid flow has a damping effect on the lateral vibration of the tube.
2. The type of support has an essential effect on the value of the natural frequency of the tube. It is shown that the natural frequency of a clamped–clamped support of composite tube is higher than that of the clamped–pinned support, the latter is higher than that of a simply support, and the simply support is higher than of clamped–free support. This can be attributed to raising the bending moment when preventing bending rotation at fixed ends.
3. Inserting intermediate support between two clamped supports does not affect the tube's natural frequency value when the length of the intermediately supported beam equals twice the length of the tube supported by two clamped end supports, shown in figure (5.4). When the length of the intermediate support tube is the same as that supported by two clamped supports, the natural frequency is doubled.

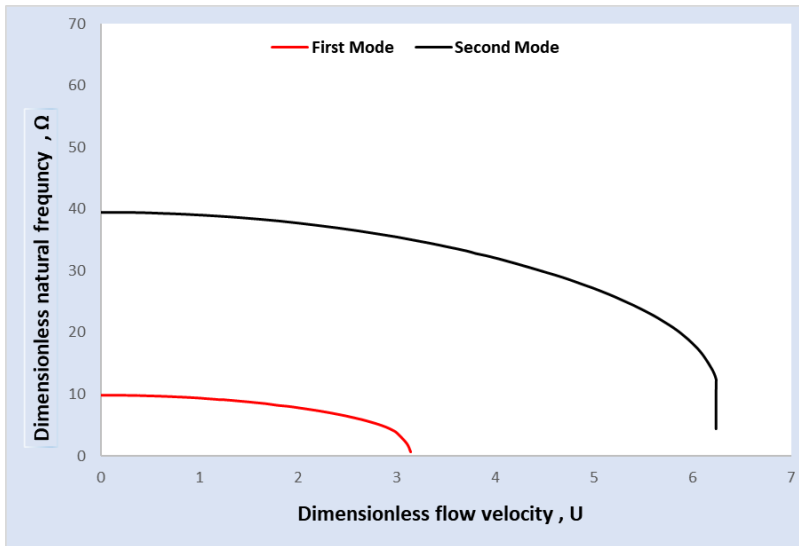


Figure (5.1). Variation of the first two natural frequencies with flow velocity for simply supported tube ($\beta=0.6336$, $\gamma=0$, $\mu=0$).

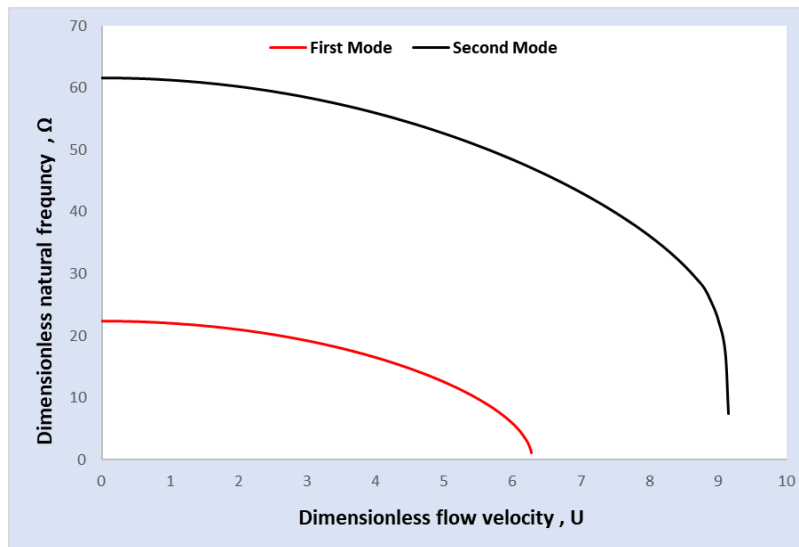


Figure (5.2). Variation of the first two natural frequencies with flow velocity for clamped-clamped tube ($\beta=0.6336$, $\gamma=0$, $\mu=0$)

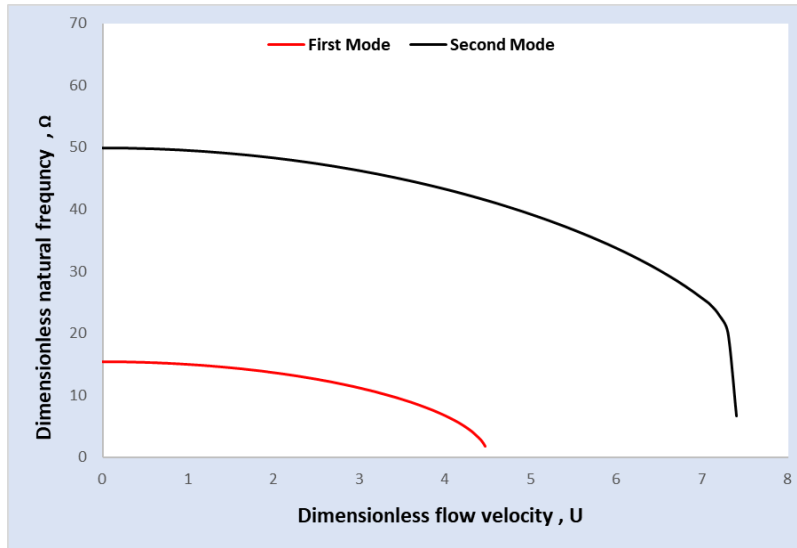


Figure (5.3). Variation of the first two natural frequencies with flow velocity for clamped – pinned supported tube($\beta=0.6336$, $\gamma=0$, $\mu=0$).

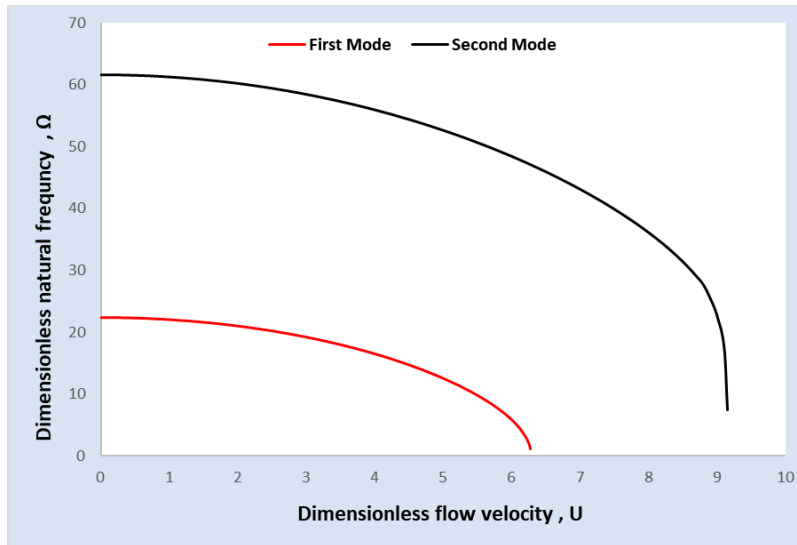


Figure (5.4). Variation of the first two natural frequencies with flow velocity for clamped – clamped tube with intermediate support ($\beta=0.6336$, $\gamma=0$, $\mu=0$).

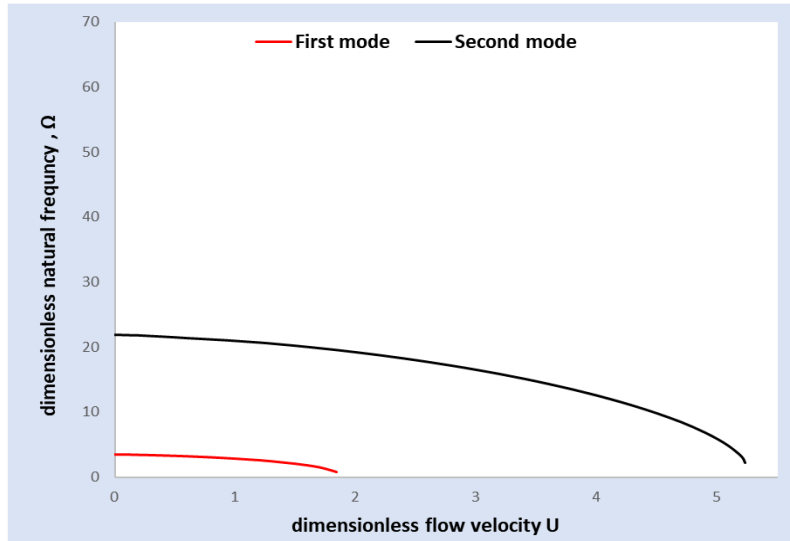


Figure (5.5). Variation of the first two natural frequencies with flow velocity for clamped–free support ($\beta=0.6336$, $\gamma =0$, $\mu=0$).

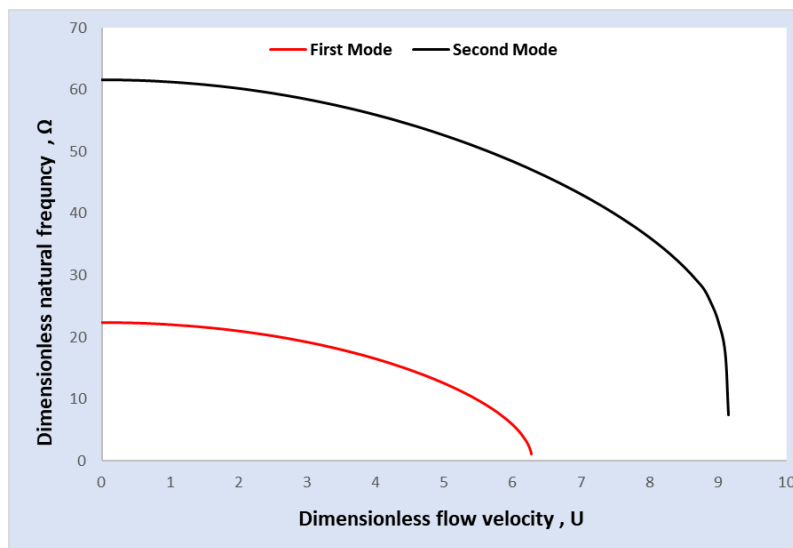


Figure (5.6). Variation of the first two natural frequencies with flow velocity for free – free support ($\beta=0.6336$, $\gamma =0$, $\mu = 0$).

5.2.2 Effect of internal damping on the natural frequency

Table (5.2) shows the values for the first mode of the natural frequency of the composite tube when the effect of internal damping and flow velocity of the fluid is zero for different boundary conditions.

Table (5.2). First mode natural frequency of composite tube including the effect of internal damping ($U = 0$, $\gamma = 0$, and $\beta = 0.6336$).

No.	Beam Configuration	$\mu=0$	$\mu=0.01$	$\mu=0.1$
1	Simply support	9.872	9.399	6.139
2	Clamped support	22.376	20.012	8.548
3	Clamped-pinned support	15.424	14.281	7.584
4	Clamped-free support	3.521	3.461	2.956
5	Free-free support	22.376	20.012	8.548

Figures (5.7 to 5.12) show the internal damping influence on the natural frequency of clamped-clamped, simply supported, clamped-pinned, clamped-clamped with simple intermediate support, clamped-free, and free-free supports.

In these figures, the internal damping effect on the dynamical behavior of the composite material tube is taken into consideration. It can be deduced that:

1. The internal damping affects the natural frequency of the tube due to the resistance to the relative motion between the material particles. The natural frequency decreased by about 4.79 %.
2. The effect of internal damping at the low flow velocity range is more than that at the high-velocity range. This behavior is attributed to the dominant damping of flowing fluid at high flow velocities.
3. When the value of the flow velocity of the fluid increases, the natural frequency gradually decreases with the increase (for any value of internal damping), then approaching a value at which the natural frequency approaches zero. The value of flow velocity that vanishes the natural frequency is called the critical flow velocity.

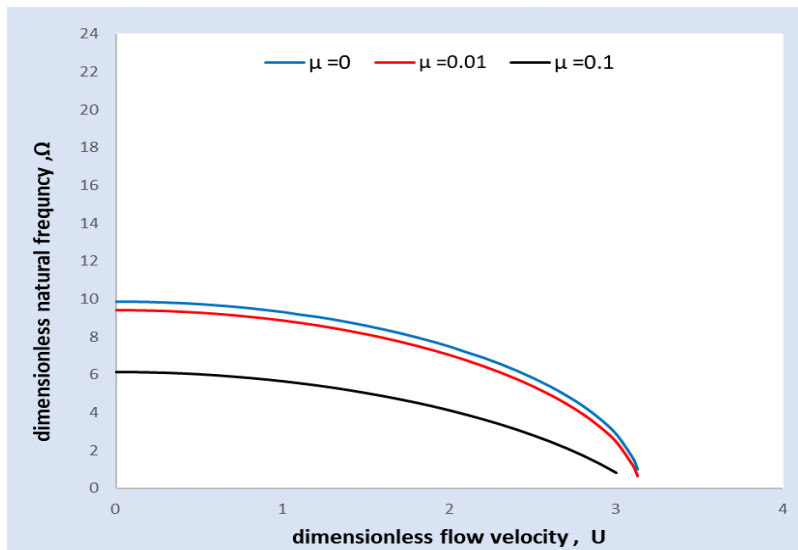


Figure (5.7). Effect of internal damping on the first mode natural frequency of a simply supported tube conveying fluid at various velocities ($\beta=0.6336$, $\gamma=0$).

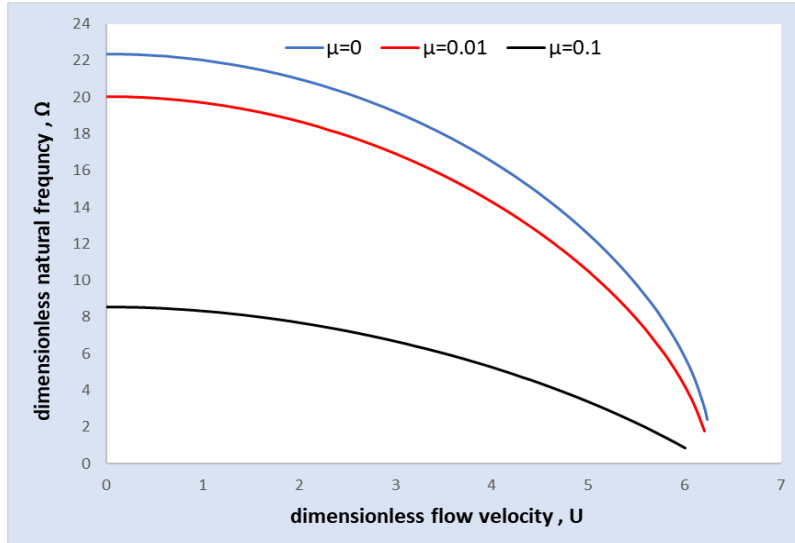


Figure (5.8). Effect of internal damping on the first mode natural frequency of a clamped supported tube conveying fluid at various velocities ($\beta=0.6336$, $\gamma=0$).

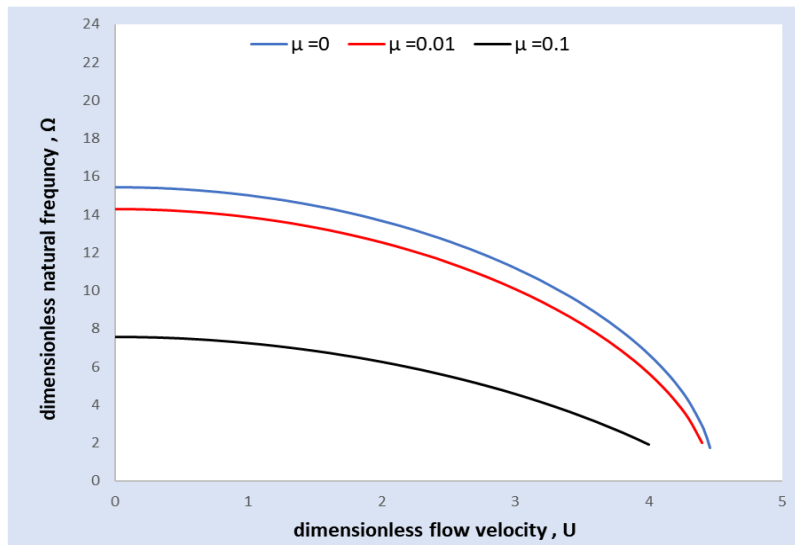


Figure (5.9). Effect of internal damping on the first mode natural frequency of a clamped-pinned tube conveying fluid at various velocities ($\beta=0.6336$, $\gamma=0$).

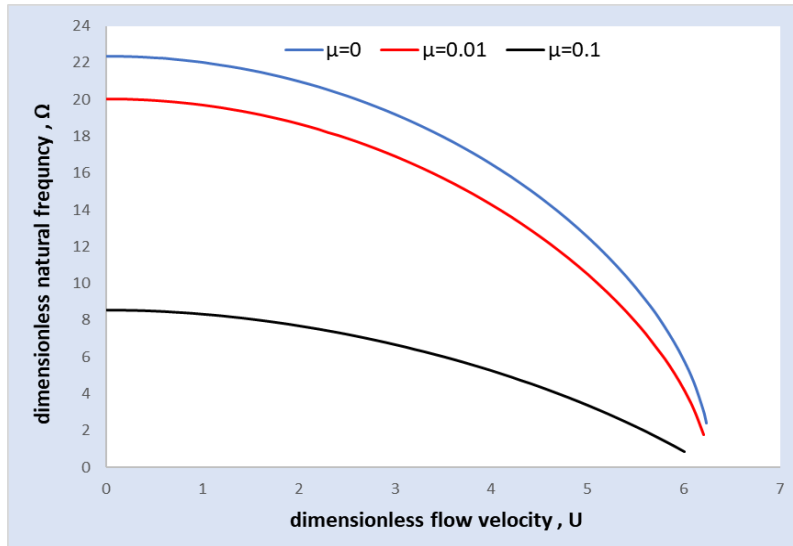


Figure (5.10). Effect of internal damping on the first mode natural frequency of a clamped-clamped tube conveying fluid with simply intermediate support ($\beta=0.6336$, $\gamma = 0$).

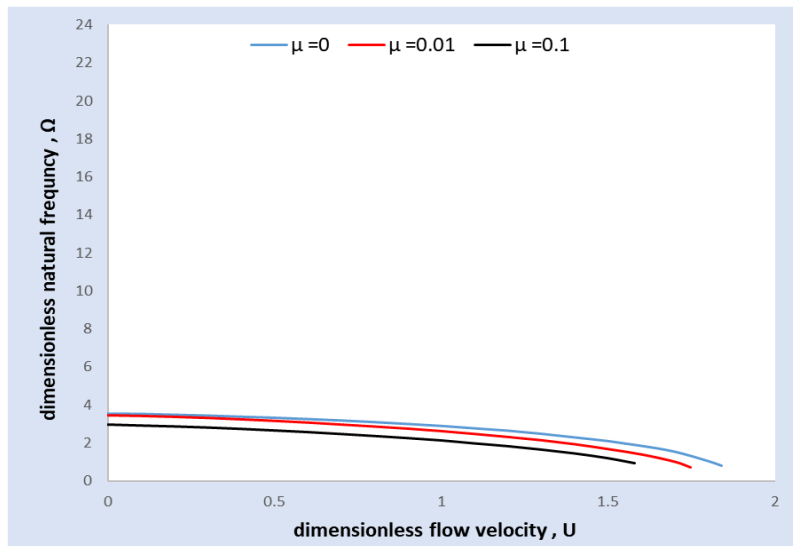


Figure (5.11). Effect of internal damping on the first mode natural frequency of clamped-free support tube conveying fluid at various velocities ($\beta=0.6336$, $\gamma = 0$).

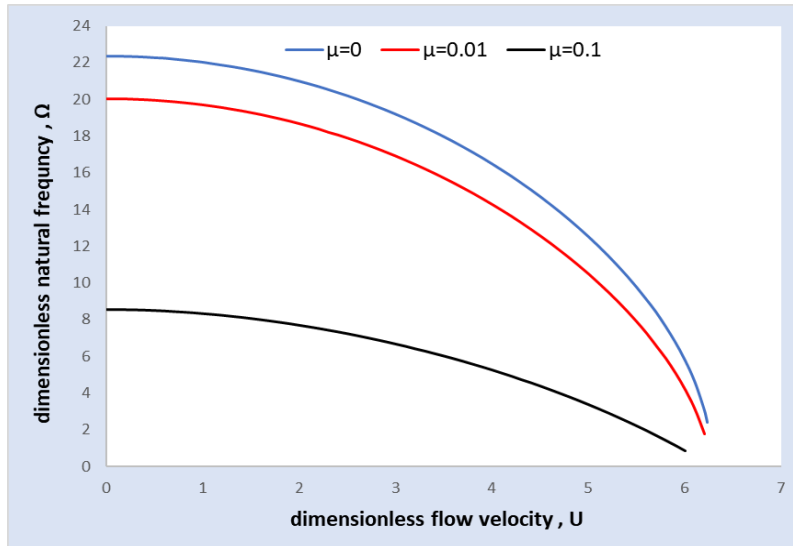


Figure (5.12). Effect of internal damping on the first mode natural frequency free-free support tube conveying fluid at various velocities ($\beta=0.6336$, $\gamma=0$).

Figures (5.13 to 5.18) are calculated for $U = (0 \text{ and } 2)$, and $\beta = 0.6336$.

These figures show that:

1. The internal damping has a non-linear effect on the natural frequency of the tube when the flow velocity is at a certain value.
2. The natural frequency decreases gradually at low values of internal damping then reaches a point that is almost close to zero when the internal damping is greater than 0.3.

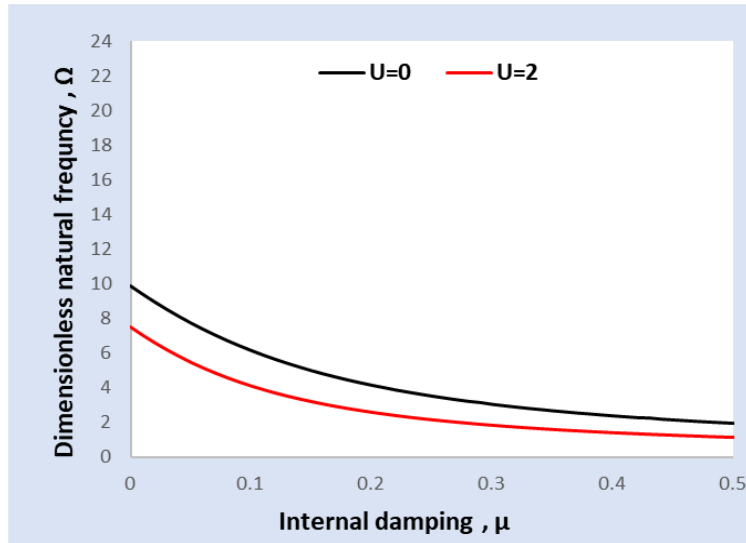


Figure (5.13). The effect of internal damping on a simply supported composite tube conveying fluid ($\beta=0.6336$, $\gamma=0$).

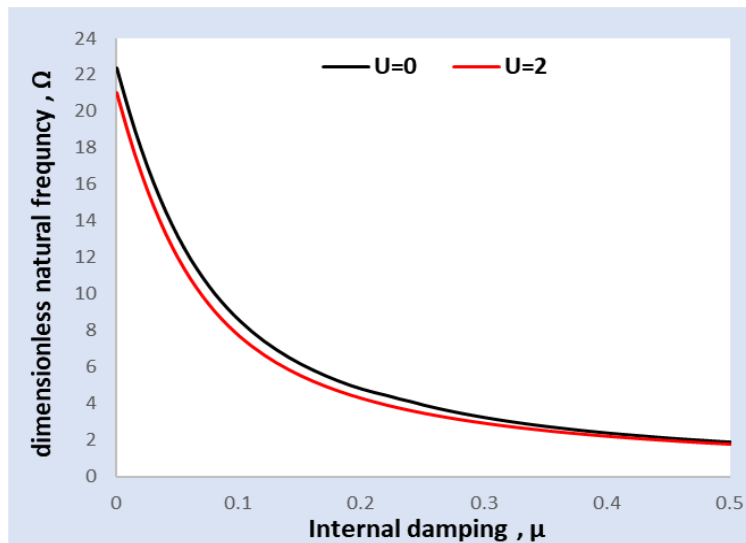


Figure (5.14). The effect of internal damping on a clamped supported composite tube conveying fluid ($\beta=0.6336$, $\gamma=0$).

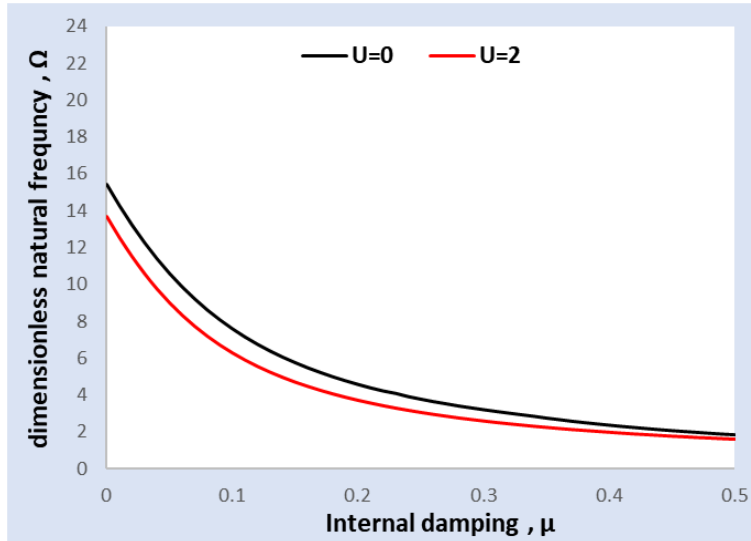


Figure (5.15). The effect of internal damping on a clamped–pinned supported composite tube conveying fluid ($\beta=0.6336$, $\gamma =0$).

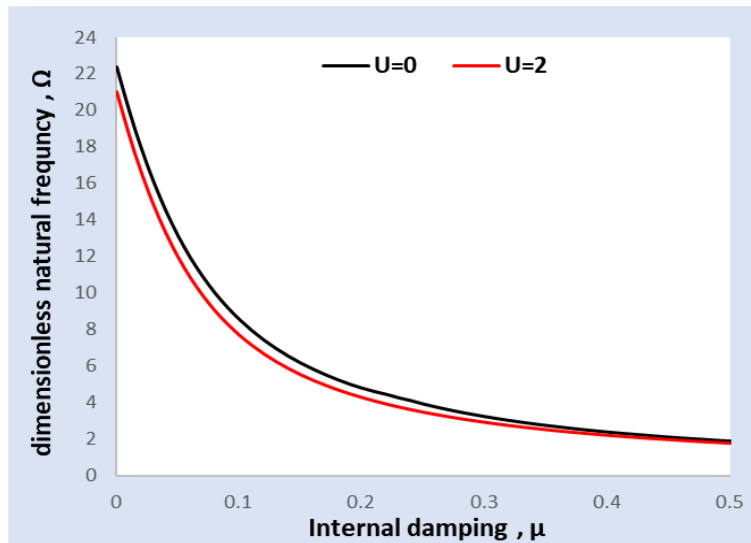


Figure (5.16). The effect of internal damping on a clamped-clamped composite tube conveying fluid with intermediate support ($\beta=0.6336$, $\gamma =0$).

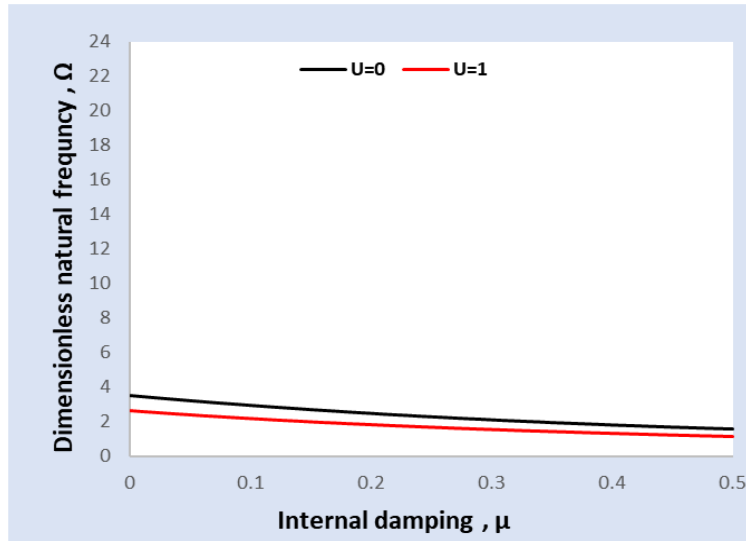


Figure (5.17). The effect of internal damping on clamped-free supported composite tube conveying fluid ($\beta=0.6336$, $\gamma =0$).

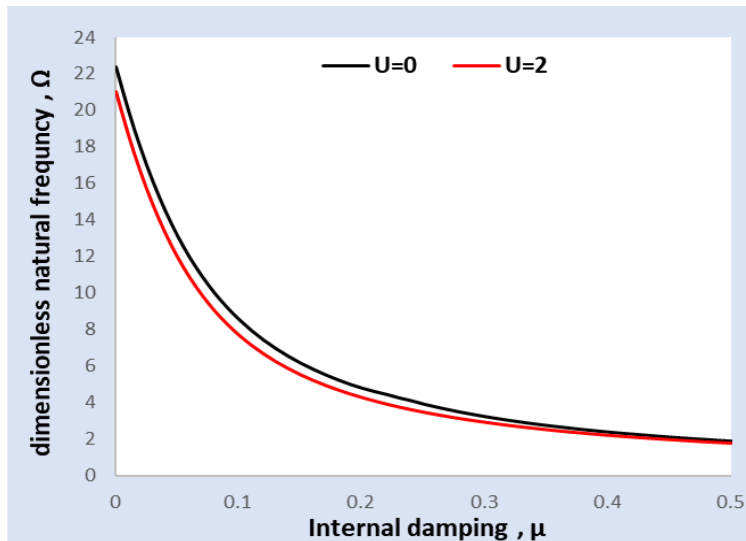


Figure (5.18). The effect of internal damping on a free – free, supported composite tube conveying fluid ($\beta=0.6336$, $\gamma =0$).

5.2.3 Effect of supporting type on the natural frequency

The natural frequency is affected by many factors, such as the increase in the flow velocity value and the internal damping.

Figure (5.19) shows the natural frequency variation with flow velocity using different supports.

An increase in the flow velocity leads to a decrease in the natural frequency until it reaches the critical flow velocity. The natural frequency approaches zero because the tube loses its stability due to the buckling phenomenon.

Figures (5.20) and (5.21) show the effect of the internal damping force and flow velocity on the natural frequency with different types of supports.

It can be seen that the increase in internal damping with increasing flow velocity decreases the natural frequency by 4.79%.

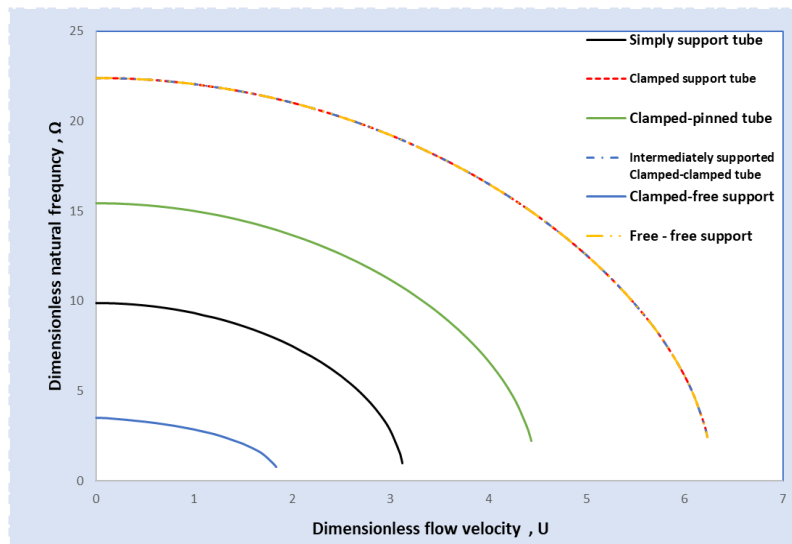


Figure (5.19). Variation of the tube first mode natural frequency with the effect of flow velocity for different supporting types at ($\beta=0.6336$, $\gamma=0$, $\mu=0$).

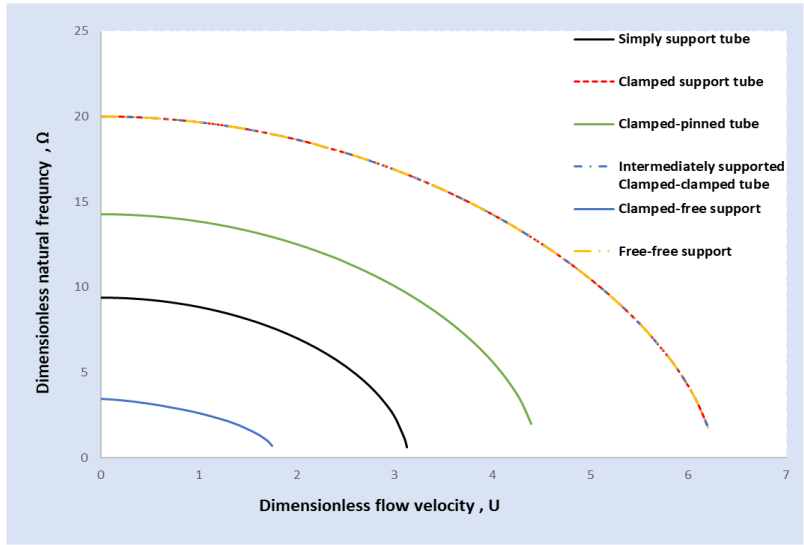


Figure (5.20). Effect of flow velocity on the tube's first mode natural frequency for different forms of supports at ($\beta=0.6336, \gamma=0, \mu=0.01$).

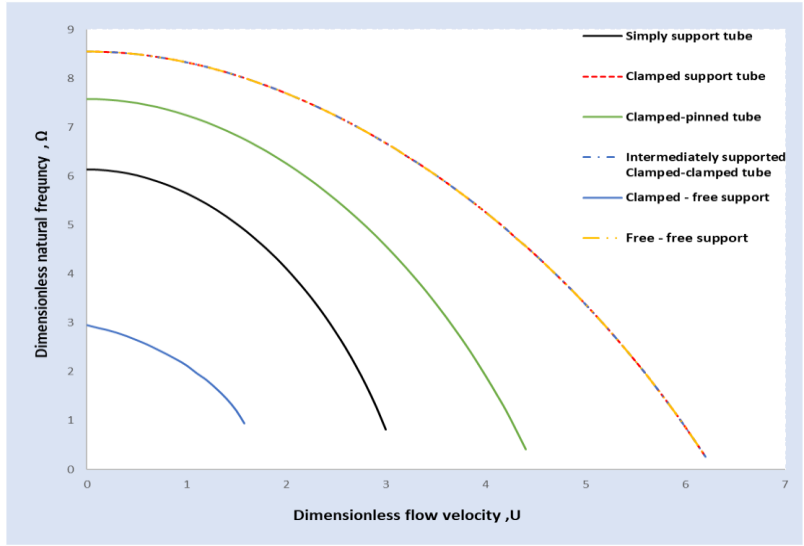


Figure (5.21). Effect of flow velocity on the tube's first mode natural frequency for different forms of supports at ($\beta=0.6336, \gamma=0, \mu=0.1$).

5.3 Experimental Results

This part deals with the experimental results obtained through measurement by the manufactured device with the rest of the auxiliary parts discussed in the third chapter and compares these practical values with the relevant theoretical results evaluated from the mathematical model presented in the second chapter. Water is used as the internal fluid passing through the tube in this work.

The readings from the apparatus include the value of the natural frequency of the exciting composite material tube and the value of flow velocity. The mean flow velocity of the flowing water is calculated from the value of the water flow rate divided by the tube internal sectional area.

Flowmeter measures the water flow rate inserted within the flow circuit. The natural frequency of the tube is recorded when the amplitude of the tubes reaches its maximum value as the speed of the exciter increases gradually from zero.

The exciter speed is measured by a laser tachometer, which gives the readings in revolution per minute. It is converted to radians per second to be comparable with the theoretical values.

The experimental values are conducted for three tubes made from the composite material.

The calculated and measured values of the tube natural frequencies are presented in Figures (5.22 to 5.24) for three types of boundary conditions.

From the theoretical and experimental results shown in the figures for the three tubes used in the test, it was found that all the experimental values are

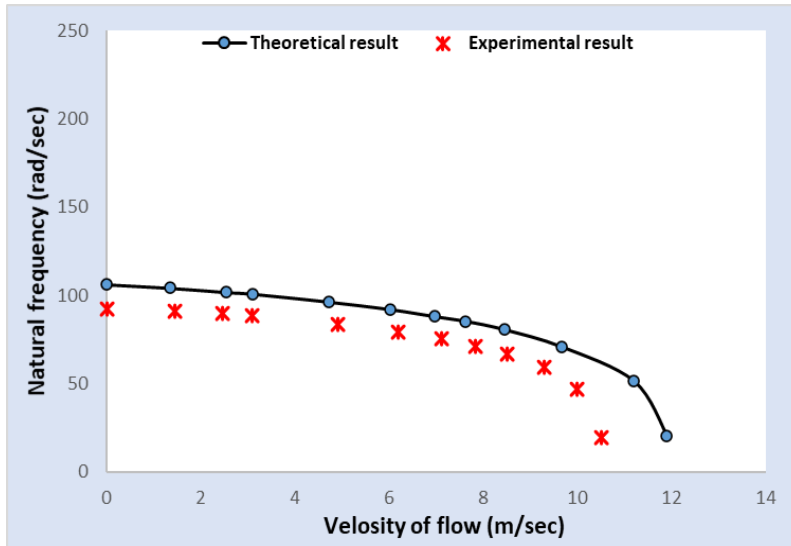
less than the corresponding theoretical results and that there is an acceptable agreement between the theoretical and practical results:

- Inaccuracy in measuring devices and errors resulting during measurements
- The supports used for supporting the tube are not ideal.

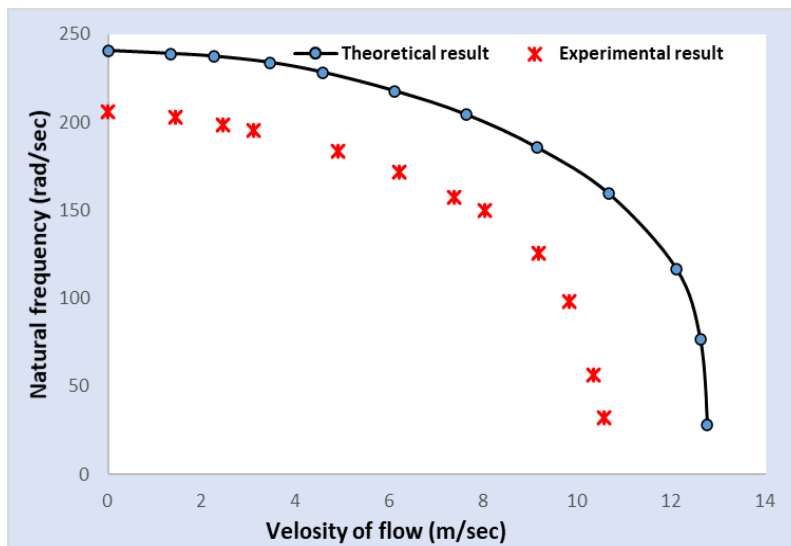
These results found that the natural frequency is affected by many factors, including the increase in the fluid flow velocity and the effect of the internal damping force of the tube material, as well as is affected by the type of supports used in the experimental application.

The three tubes are made from the carbon-fiber epoxy composite. The modulus of elasticity is 2.6 Gpa.

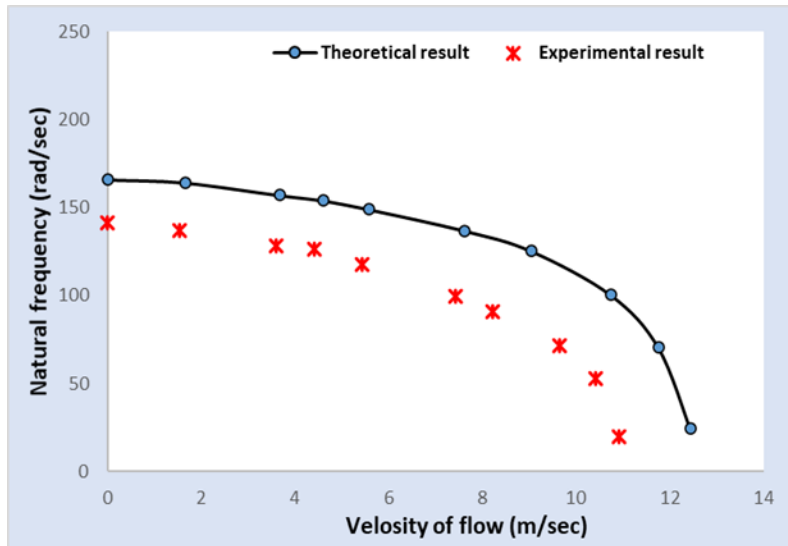
For the first tube, the outer diameter is 0.023 m, the inner diameter is 0.013 m, the thickness is 0.005 m, the mass of the 0.02 m long piece is 0.012 kg. Figure (5.22) shows the relationship between the natural frequency and fluid velocity in the first mode for three boundary conditions.



(a) simply support



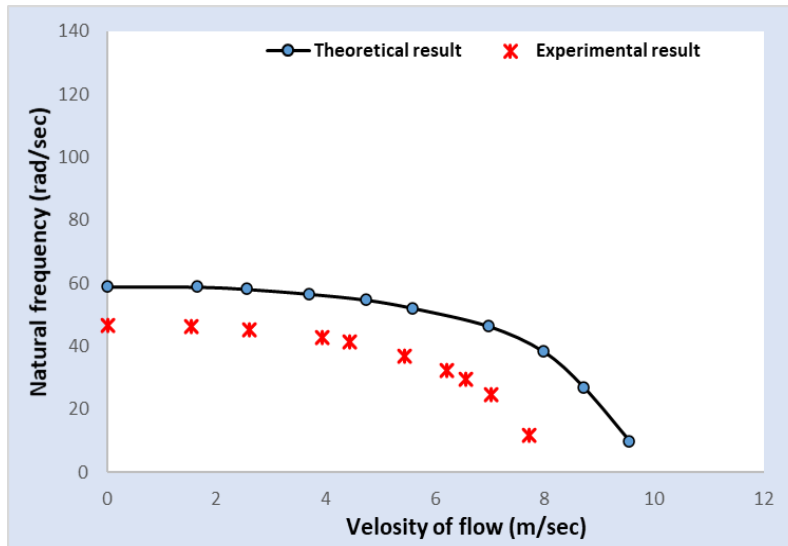
(b) clamped support



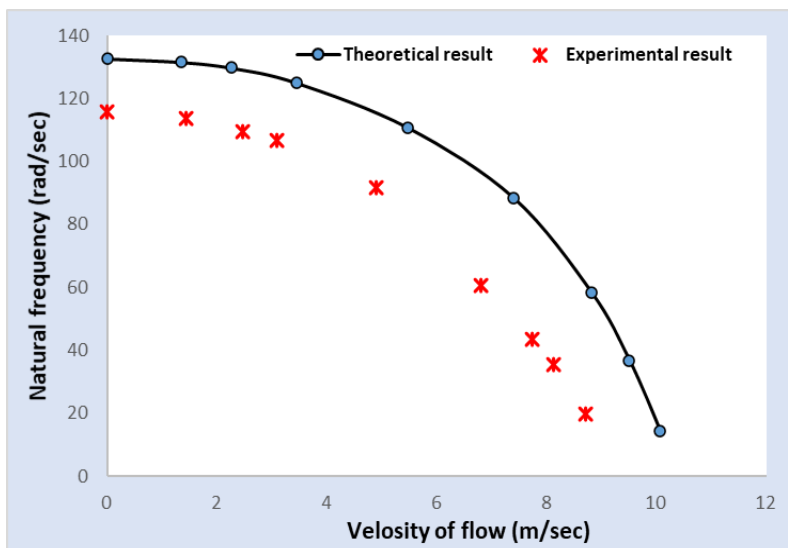
(c) clamped – pinned support

Figure (5.22/a, b, c). Experimental and theoretical effects of flow velocity on the tube's first mode natural frequency for the first tube ($\beta=0.6336, \gamma=0, \mu=0$).

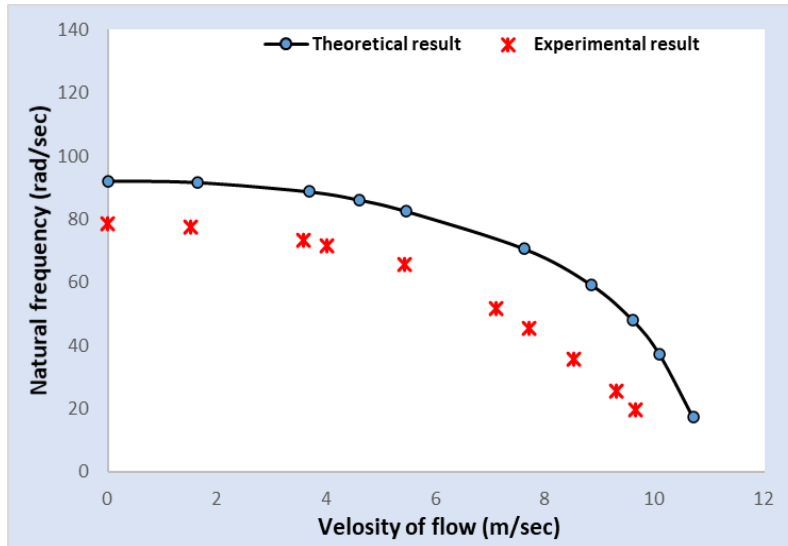
For the second tube, the outer diameter is 0.015 m, the inner diameter is 0.007 m, the thickness is 0.004 m, the mass of the 0.02 m long piece is 0.007 kg. Figure (5.23) shows the relationship between the natural frequency and fluid velocity in the first mode for three boundary conditions.



(a) simply support



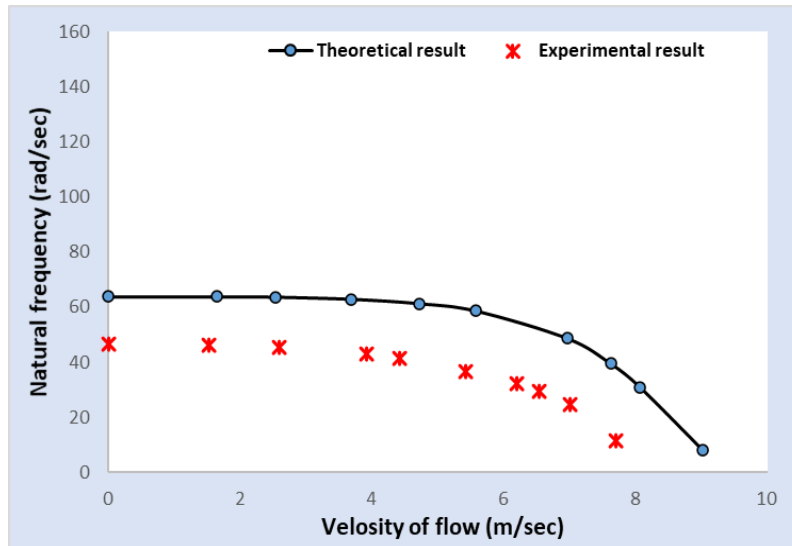
(b) clamped support



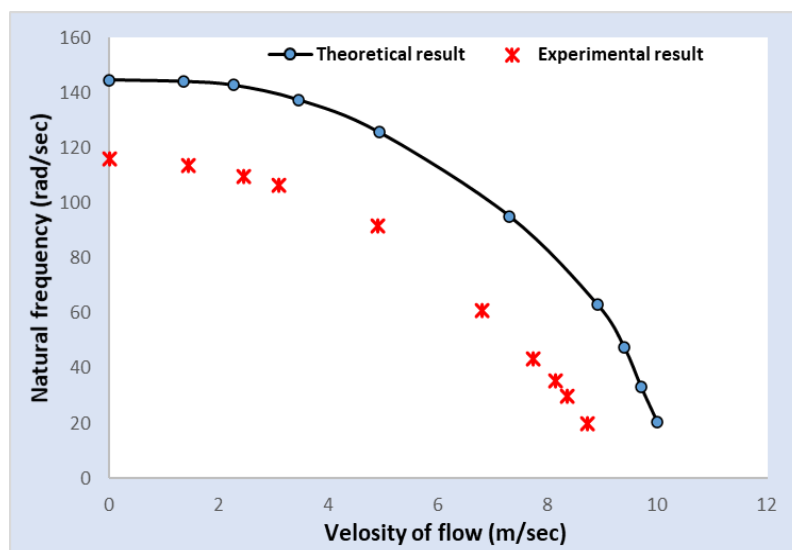
(c) clamped – pinned support

Figure (5.23/a, b, c). Experimental and theoretical effects of flow velocity on the tube's first mode natural frequency for the second tube ($\beta=0.6336$, $\gamma=0$, $\mu=0$).

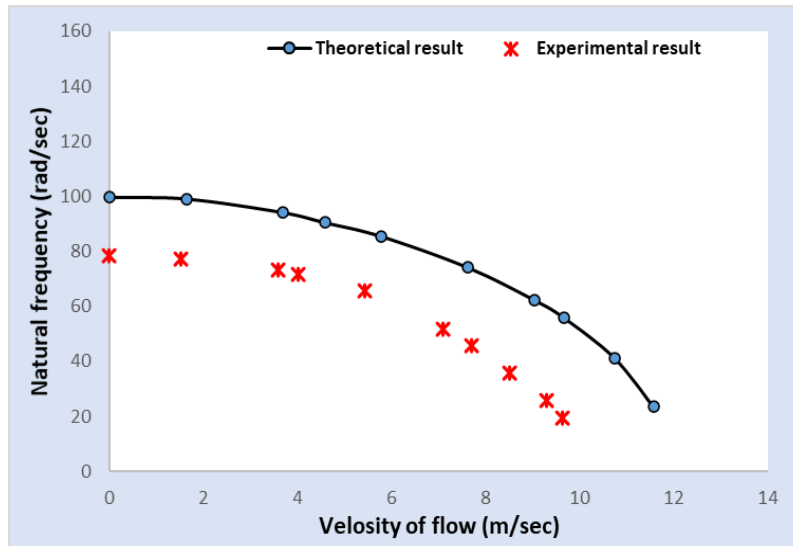
For the third tube, the outer diameter is 0.013 m, the inner diameter is 0.007 m, the thickness is 0.003 m, the mass of the 0.02 m long piece is 0.003 kg. Figure (5.24) shows the relationship between the natural frequency and fluid velocity in the first mode for three boundary conditions.



(a) simply support

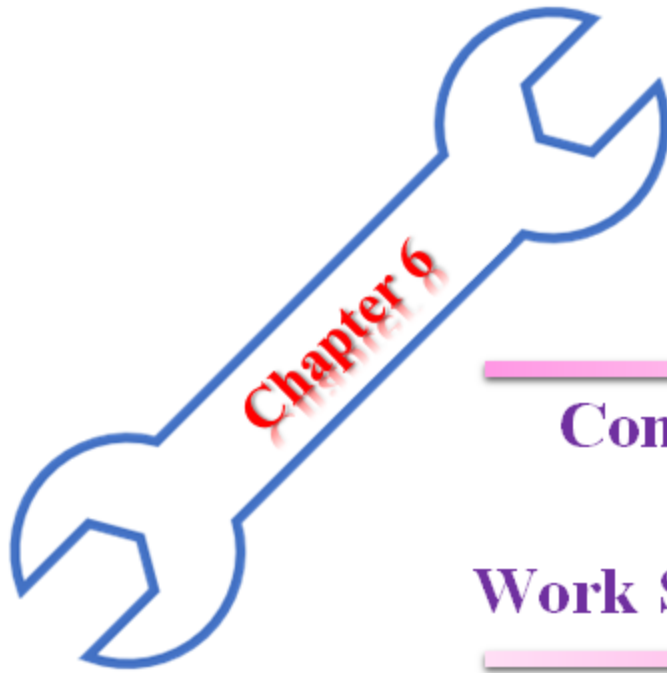


(b) clamped support



(C) clamped – pinned support

Figure (5.24/a, b, c). Experimental and theoretical effects of flow velocity on the tube first mode natural frequency for the third tube ($\beta=0.6336$, $\gamma=0$, $\mu=0$).



**Conclusions
&
Work Suggestions**



Chapter Six

Conclusions and Work Suggestions

6.1 Introduction

This chapter deals with the conclusions obtained from the present study. It also provides some recommendations and suggestions which may be useful for future works.

6.2 Conclusions

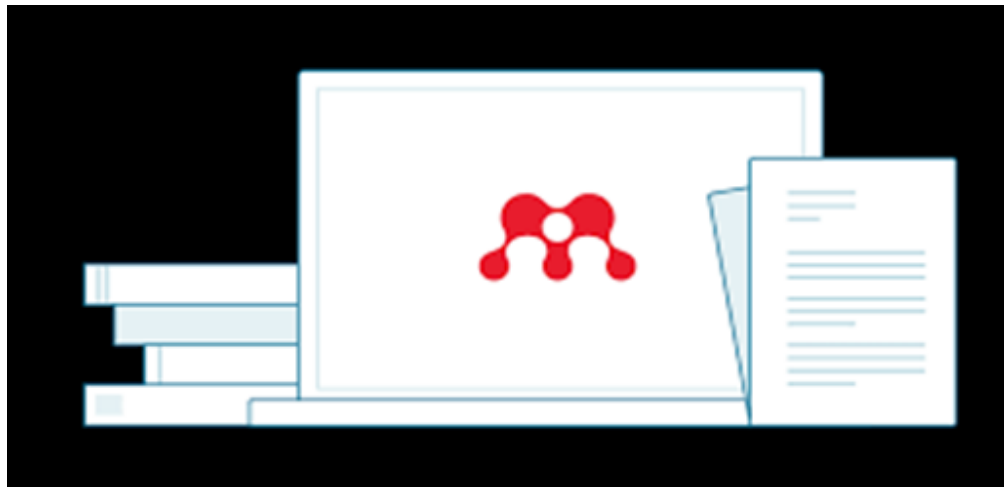
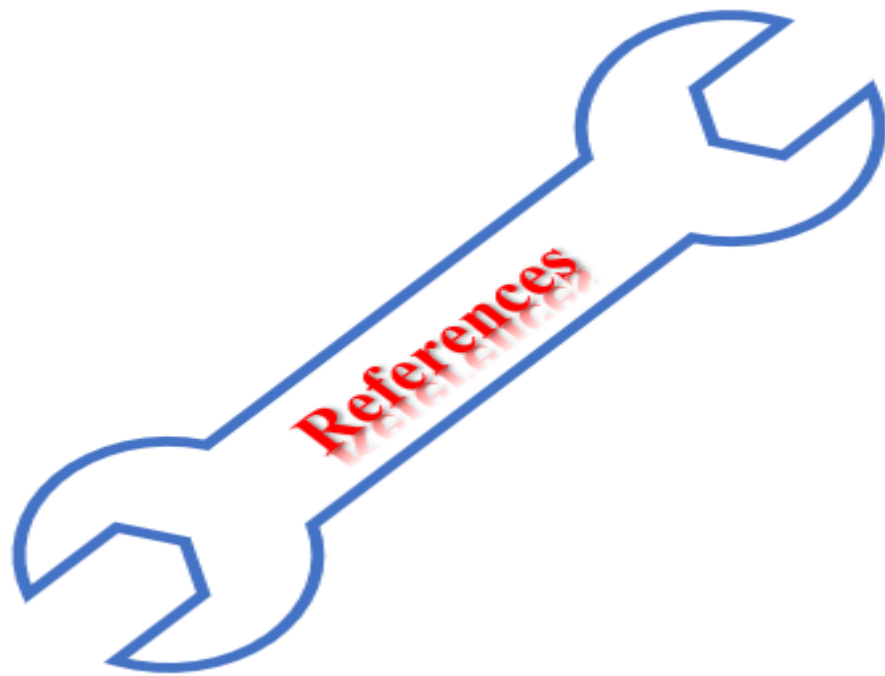
1. Flow velocity factor plays an important role in the value of free vibration of composite tubes. Depending on type ends conditions, it may cause instability to the tube when reaching a certain value.
2. The flow velocity value of the fluid reduces the value of the natural frequency of the free vibration of the composite material tube, which means that the tube loses its stability due to the phenomenon of buckling, as the natural frequency decreases gradually until a point approaching zero called the "critical velocity value". Also, the flow velocity reduces the vibration amplitude due to the damping delivered by fluid forces.
3. The effect of fluid flow velocity at lower velocities is small compared to higher velocities. This trend is seen for all types of boundary conditions. The type of boundary conditions significantly affects the value of the natural frequency. It is shown that the natural frequency of a clamped support of composite tube is higher than that of the clamped-pinned support, the latter is higher than that of a simply support, and the simply support higher than of

clamped-free support. This behavior referred to the effects of the bending moment raised when preventing bending rotation at fixed ends.

4. Inserting intermediate support between two clamped supports does not affect the tube's natural frequency value when the length of the intermediately supported beam equals twice the length of the tube supported by two clamped end supports. When the length of the intermediate support tube is the same as that supported by two clamped supports, the natural frequency is doubled.
5. The internal damping affects the natural frequency by up to 4.79 % when the internal damping increases by 0.01% due to the resistance to the relative motion between the material particles.
6. The effect of internal damping at the low-velocity range is more than that at the high-velocity range. This behavior is attributed to the dominant damping of flowing fluid at high flow velocities.

6.3 Future Work Suggestions

- 1- Analyzing the same problem using the method of characteristics.
- 2- Studying the dynamics of tubes conveying fluid, considering the viscous damping and the temperature.



References

- [1] Rock West, February 2018. "Materials Used to Manufacture Composite Tubing" (<https://www.rockwestcomposites.com/blog/materials-used-to-manufacture-composite-tubing/>).
- [2] Paidoussis M.P. and Issid N.T., 1974. "Dynamic stability of pipes conveying fluid". *Journal of Sound and Vibration* , vol.33, p.267–294.
- [3] Long Liu and Fuzhen Xuan, 2010"Flow-Induced Vibration Analysis of Supported Pipes Conveying Pulsating Fluid Using Precise Integration Method", *Journal of Mathematical Problems in Engineering*, vol.2010, Article ID 806475, . <https://doi.org/10.1155/2010/806475>
- [4] Huang Yi-min, Liu Yong-shou, Li Bao-hui, Li Yan-jiang and Yue Zhu-feng, 2010."Natural frequency analysis of fluid conveying pipeline with different boundary conditions". *Journal of Nuclear Engineering and Design*, vol.240 , Issue 3 ,Pages461-467, ISSN 0029-5493,<https://doi.org/10.1016/j.nucengdes.2009.11.038>.
- [5] Ahmed A. Al-Rajihy and Hazim U. Alwan, July 2010. "The Dynamical Behavior of Y-Shaped Tubes Conveying Fluid" , ASME 2010 10th Biennial Conference on Engineering Systems Design and Analysis Istanbul, Turkey Paper No:ESDA2010-24101, pp.23-27 ,<https://doi.org/10.1115/ESDA2010-24101>
- [6] Nabeel K. Abid Al-Sahib,Adnan N. Jameel and Osamah F. Abdulateef, June 2010. "Investigation into the Vibration Characteristics and Stability of a Welded Pipe Conveying Fluid". *Jordan Journal of Mechanical and Industrial Engineering* . vol. 4, Number 3, ISSN 1995-6665 Pages 378 - 387.

- [7] Mahmud Rasheed Ismail, January 2011. "Evaluating The Dynamical Behavior And Stability of Pipes Conveying Fluid" Thesis for: PhD Al-Nahrain University. DOI:10.13140/RG.2.2.34510.87369
- [8] T.G.Ritto, C.Soize, F.A.Rochinha and Rubens Sampaio, 2014 " Dynamic stability of a pipe conveying fluid with an uncertain computational model", Journal of Fluids and Structures, Volume 49, Pages 412-426, ISSN 0889-9746, <https://doi.org/10.1016/j.jfluidstructs.2014.05.003>.
- [9] Ahmet Kesimli, Süleyman Murat Bağdatlı and Seyit Çanakçı, 2016. "Free vibrations of fluid conveying pipe with intermediate support". Journal of Engineering Structures & Materials ,vol.2, p.75-87.
- [10] Ahmed Al-Rajihy and Mohanned Kadhom , Feb. 2018. "Analysis of Bending Response of Tubes Conveying Fluid by the Method of Characteristics". Journal of Advances in Natural and Applied Sciences, (vol.12, Issue 2)
- [11] Salah Noori Alnomani 2018. "Investigation of vibration characteristics for simply supported pipe conveying fluid by mechanical spring". ARPN Journal of Engineering and Applied Sciences vol.13, No.11, ISSN 1819-6608
- [12] Sutar, Shankarachar , Madabhushi, Radhakrishna , Chellapilla, Kameswara Rao , Poosa, Ramesh Babu , June 2019. "Determination of Natural Frequencies of Fluid Conveying Pipes using Muller's Method". Journal of The Institution of Engineers (India): Series C, vol.100, Issue 3, pp.449-454. doi: 10.1007/s40032-018-0446-6.
- [13] Wasiu A. Oke, Yehia A. Khulief, 2018 "Effect of internal surface damage on vibration behavior of a composite pipe conveying fluid", Journal of Composite Structures, vol.194, Pages:104-118, ISSN 0263-

8223, <https://doi.org/10.1016/j.compstruct.2018.03.098>.

[14] Gyula Szabó, Károly Váradi and Dávid Felhős. February 2018. "Bending Analysis of a Filament-Wound Composite Tube" , Journal of Modern Mechanical Engineering , vol.8, No.1

[15] Wasiiu A. Oke, Yehia A. Khulief, July 2020. "Dynamic Response Analysis of Composite Pipes Conveying Fluid in the Presence of Internal Wall Thinning" , Journal of Engineering Mechanics ,vol.146, Issue 10 , [https://doi.org/10.1061/\(ASCE\)EM.1943-7889.0001842](https://doi.org/10.1061/(ASCE)EM.1943-7889.0001842)

[16] H.L. Dai, L. Wang and Q. Ni, 2013 "Dynamics of a fluid-conveying pipe composed of two different materials", International Journal of Engineering Science, vol.73, Pages:67-76, ISSN 0020-7225, <https://doi.org/10.1016/j.ijengsci.2013.08.008>.

[17] Nawal H. Al – Raheimy (2016) "Free Vibrations of Uniform Pipes Made From Composite Materials at an Internal Flow Under Effect of Additional Boundary Conditions " Journal of Babylon University/Engineering Sciences, vol.24, No. 3

[18] B. A. Khudayarov, KH. M. Komilova and F. ZH. Turaev, 2019. " Numerical Simulation of Vibration of Composite Pipelines Conveying Pulsating Fluid", International Journal of Applied Mechanics vol.11, No. 9 doi: 10.1142/S175882511950090X

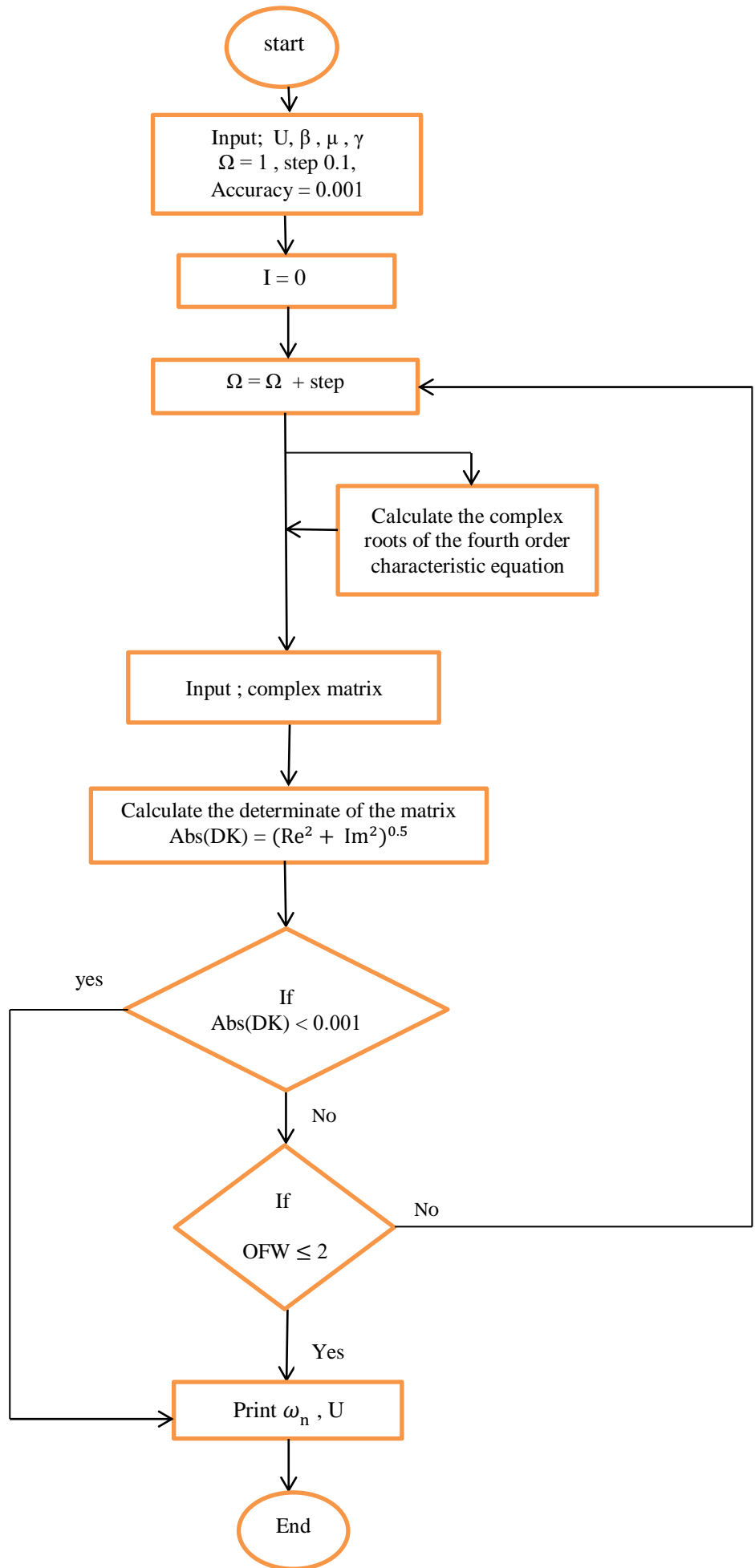
[19] M.I. Geuchy Ahmad and S.V. Hoa, 2016 "Flexural stiffness of thick walled composite tubes", Journal of Composite Structures, vol.149, Pages 125-133,ISSN0263-8223,<https://doi.org/10.1016/j.compstruct.2016.03.050>.

[20] K.Y. Maalawi , A. M. Abouel-Fotouh , M. El Bayoumi and Khaled Ahmed Ali Yehia , 2016. "Design of Composite Pipes Conveying Fluid for Improved Stability Characteristics". International Journal of Applied Engineering Research ISSN 0973-4562 , vol.11, N0.12 pp7633-7639

- [21] Oke, W.A., Khulief, Y.A. , February 2016. "Vibration analysis of composite pipes using the finite element method with B-spline wavelets". *Journal of Mechanical Science and Technology* , vol.30, pp.623–635, <https://doi.org/10.1007/s12206-016-0116-7>
- [22] B.A. Khudayarov, Kh.M. Komilova , F.Zh. Turaev and J.A. Aliyarov, January 2020 " Numerical simulation of vibration of composite pipelines conveying fluids with account for lumped masses", *International Journal of Pressure Vessels and Piping* ,Volume 179, <https://doi.org/10.1016/j.ijpvp.2019.104034>
- [23] Chimanbhai Magandas Patel , (1969) "Vibration of an internally damped tapered truncated cantilever beam".Masters Theses. [https://scholarsmine.mst.edu/Masters Theses/6982](https://scholarsmine.mst.edu/Masters%20Theses/6982)
- [24] D. Kroisová ,2010 "An Internal Damping in Epoxy Composite Systems" , *Journal of Health & Environmental Research Online (HERO)*, Page Numbers 1207-1217
- [25] L. Wang, H.L. Dai, Q. Qian, 2012 "Dynamics of simply supported fluid-conveying pipes with geometric imperfections", *Journal of Fluids and Structures*, vol.29, Pages 97-106, ISSN 0889-9746, <https://doi.org/10.1016/j.jfluidstructs.2011.12.013>.
- [26] Colakoglu Mehmet ,2012."Factors effecting internal damping in aluminum" , *Journal of Theoretical and Applied Mechanics*, vol.42, no.1, p.95-105, ISSN 1429-2955. <http://www.ptmts.org.pl/jtam/index.php/jtam/article/view/v42n1>.
- [27] Seniha Karic, Avdo Voloder, Rusmir Bajric and Dzafer Kudumovic, January 2012."Determination of the Internal Damping Coefficient in an Elastic Clamping Beam" , *Technics Technologies Education Management* 7(4):1468-1471.

- [28] K.I.Mohammed, 2017. "Dynamic Behavior of Cracked Pipe Conveying Fluid Using Different End Conditions " Masters Theses, Kerbala University.
- [29] Ivan Grant , 2010 ." Flow Induced Vibrations in Pipes: a Finite Element Approach " Masters Theses, Cleveland State University.
- [30] Mohammad Irshad Ali and J. Anjaneyulu ,2018 ." Effect of fiber-matrix volume fraction and fiber orientation on the design of composite suspension system ", IOP Conf. Series: Materials Science and Engineering 455 (2018) 012104 , doi:10.1088/1757-899X/455/1/012104
- [31] William T. Thomson,"Theory of Vibration with Application." , McGraw. Hill, 1986, p. 283.

Appendix A:



ملخص الرسالة

عادة ما تكون الأنابيب المركبة مصنوعة من مادتين مركبتين أو أكثر. يمكن استخدام هذه الأنابيب لخطوط الوقود والأنابيب الهيدروليكية والاستخدامات المنزلية والصناعية.

في الدراسة الحالية، تم استخدام أكثر أنواع المواد المركبة شيوعاً لتصنيع الأنبوب وهو ألياف الكربون - الإيبوكسي. يستخدم على نطاق واسع بسبب خصائصه المهمة، بما في ذلك المقاومة العالية للوزن والمتانة الجيدة والأسعار المناسبة.

بسبب الميل إلى استخدام أنابيب ناجحة مع اهتزاز أقل ومعدل تآكل منخفض، تم توجيه هذه الدراسة إلى السلوك الديناميكي للأنابيب المصنوعة من المواد المركبة التي تنقل السوائل.

تم تقديم التقييم المنهجي للجوانب الأساسية للسلوك الديناميكي للأنبوب المصنوع من المادة المركبة مع تأثير سرعة التدفق والتخميد الداخلي على الاهتزاز الحر للأنبوب المصنوع من المادة المركبة، والذي يمثل العامل الرئيسي في هذا العمل، باستخدام أنواع مختلفة من الشروط الحدودية.

تم حل النموذج الرياضي للأنبوب المركب تحليلياً لحساب تأثير المعلمات والمتغيرات ذات الصلة. تم تقديم النتائج النظرية في شكل لا أبعاد لها مع الخصائص الميكانيكية.

تم تحديد التردد الطبيعي في الجزء النظري من خلال اشتقاق المعادلة الحاكمة باستخدام نظرية أويلر-برنولي واستبدال الشروط الحدودية في المعادلة لاستخراج جذور المعادلة متعددة الحدود وكتابتها في شكل مصفوفة وكتابتها في برنامج (Q-basic) لتحديد قيمة التردد الطبيعي.

وجد أن زيادة سرعة التدفق تؤدي إلى انخفاض التردد الطبيعي تدريجياً. زاد معدل النقص حتى كانت قيمة التردد الطبيعي تقارب الصفر عند نقطة تسمى "سرعة التدفق الحرجة" وهي سرعة التدفق التي ينخفض عندها التردد الطبيعي. وجد أن الأنبوب المركب المدعوم بدعم بسيط له سرعة تدفق حرجة لا بعدية تبلغ 3.12. على النقيض من ذلك، فإن الأنبوب المركب المدعوم بدعم محكم له سرعة تدفق حرجة لا بعدية تبلغ 6.23، وسرعة التدفق الحرجة اللابعدية للأنبوب المدعوم بدعم بسيط مع دعم محكم هي 4.42. كانت هذه النتائج بدون أخذ تأثير معامل التخميد الداخلي.

وفقاً للنتائج النظرية، زادت سرعة التدفق الحرجة عند زيادة وضع الاهتزاز. علاوة على ذلك، فإن سرعة التدفق الحرجة للأنبوب المدعوم بدعم محكم أعلى بنسبة 50% من سرعة التدفق الحرجة للأنبوب المركب المدعوم بدعم بسيط. يؤثر التخميد الداخلي على التردد الطبيعي بنسبة تصل إلى 4.79% عندما يزيد التخميد الداخلي بنسبة 0.01%.

في الجزء التجريبي تم تصنيع جهاز لتأكيد النتائج النظرية لحساب التردد الطبيعي من خلال استخدام مقياس سرعة الدوران لتحديد سرعة دوران العمود المرفقي، حيث تمثل عدد الدورات المعروضة على الشاشة الرقمية للجهاز قيمة التردد الطبيعي العملي للأنبوب المصنوع من المواد المركبة ومقارنة النتائج التجريبية مع النتائج النظرية.



جمهورية العراق
وزارة التعليم العالي
جامعة كربلاء - كلية الهندسة
قسم الهندسة الميكانيكية

دراسة عملية ونظرية لامتناهات أذاريبج الراتنج المدعمة باللياف الكاربون الناقل للموائج

رسالة

مقدمة لقسم الهندسة الميكانيكية / جامعة كربلاء
وهي جزء من متطلبات الحصول على درجة
ماجستير علوم في الهندسة الميكانيكية
(ميكانيك تطبيقي)

من قبل

ساره سالم حسن

بكالوريوس العلوم في الهندسة الميكانيكية (2017 م)

اشراف

أ.د. أحمد عبد الله الراجحي
م.د. باسم رحيم صادق